Untersuchungen zu Implantat-assoziierten Knocheninfektionen durch *Staphylococcus aureus*

Inaugural-Dissertation

zur Erlangung des Doktorgrades
der Mathematisch-Naturwissenschaftlichen Fakultät
der Heinrich-Heine-Universität Düsseldorf

vorgelegt von

Ceylan Daniela Windolf
aus Frankfurt am Main

Düsseldorf, Juni 2015

aus dem Institut für Medizinische Mikrobiologie und Krankenhaushygiene
der Heinrich-Heine-Universität Düsseldorf

Gedruckt mit der Genehmigung der
Mathematisch-Naturwissenschaftlichen Fakultät der
Heinrich-Heine-Universität Düsseldorf

Referent: Univ.- Prof. Dr. med. Klaus Pfeffer

Korreferent: Univ.- Prof. Dr. Johannes Hegemann

Tag der mündlichen Prüfung: 30.10.2015

Bei der vorliegenden kumulativen Promotion handelt es sich um eine verkürzte Darstellung der Modelletablierungen und Forschungsergebnisse. Eine ausführliche Darstellung wurde in folgenden Fachzeitschriften publiziert:

Windolf CD, Meng W, Lögters TT, MacKenzie CR, Windolf J, Flohé S (2013) Implant-Associated Localized Osteitis in Murine Femur Fracture by Biofilm Forming *Staphylococcus aureus*. A Novel Experimental Model. J Orthop. Res. 31(12):2013–2020.

Windolf CD, Lögters TT, Scholz M, Windolf J, Flohé S (2014) Lysostaphin-Coated Titan-Implants Preventing Localized Osteitis by *Staphylococcus aureus* in a Mouse Model. PloS One 9(12):e115940

Für die Liebe meines Lebens

Inhaltsverzeichnis

Einleitung

Die Implantat-assoziierte Infektion stellt trotz aller chirurgischer Interventionen, moderner OP-Verfahren, präoperativer Antibiotika-Prophylaxe und ggf. post-operativer Antibiotika-Gabe ein immenses Problem bei der Versorgung von Knochenbrüchen dar [1]. Etwa 2/3 aller Implantat-assoziierten Infektionen sind auf Staphylokokken zurückzuführen. Je etwa 1/3 entfallen dabei auf *Staphylococcus epidermidis* (SE), der auf Kunststoffmaterialien wie Kathetern siedelt, und *Staphylococcus aureus* (SA), der bevorzugt auf Metallen anheftet [1–4]. 42,7 % aller Wundinfektionen in Unfallchirurgie und Orthopädie sind mit *Staphylococcus aureus* assoziirt [5], allein 3,5 % der tiefen Infektionen entfallen dabei auf die distale Tibiaplatte [6]. Pathogene wie SE oder SA siedeln auf der Haut und auf verschiedenen Schleimhäuten wie dem Nasen-Rachen-Raum [7, 8]. Die Rate der Träger von SA bei gesunden Erwachsenen in der deutschen Bevölkerung liegt zwischen 15% und 40%, wobei Personen, die z.B. beruflich exponiert sind, eine höhere Trägerrate aufweisen [9]. Durch Frakturen mit schwerwiegenden Weichteilverletzungen oder bei ausgedehnten orthopädisch-traumatologischen Operationen können die Keime tief in die Wunde gelangen und dort zu schweren Infektionen führen. Bakterien heften sich an das Implantat an, vermehren sich dort und bilden einen Biofilm, der sie vor der Immunantwort schützt und die Antibiotikaresistenz steigert [10–12]. Hydrophobe / hydrophile und elektrostatische Eigenschaften, Van der Waals-Kräfte sowie das SA-spezifische Autolysin/Adhesin Protein AtlA sind entscheidend für die primäre Anheftung an Oberflächen verantwortlich [2, 13]. Mit Hilfe von Oberflächenproteinen, genannt MSCRAMMs (microbial surface components recognizing adhesive matrix molecules) siedeln sich die Bakterien auf der Implantat-Oberfläche an, vermehren sich und bilden mehrere Schichten aus. Bei der daraus resultierenden Zell / Zell Adhäsion,

die durch PIA (polysaccharide intercellular adhesin) unterstützt wird, startet die Expression einer Vielzahl von bakteriellen Genen, die Proteine zur Biofilmbildung kodieren [13–15]. Hat sich ein Biofilm gebildet, ist es schwer, die Bakterien mit chirurgischen Interventionen wie Lavage und Debridement oder mit lokalen und / oder systemisch verabreichten Antibiotika zu bekämpfen. Ausgeschüttete Proteine der Biofilm-Matrix locken Leukozyten an und bewirken eine lokale Immunantwort. Polymorphkernige Granulozyten (PMNs), Zellen in der ersten Verteidigungslinie der angeborenen Immunantwort und ausgeschüttete Entzündungsfaktoren zerstören den Knochen und das umgebende Gewebe, ohne die Infektion wirksam zu bekämpfen [16–18].

Die frühzeitige Erkennung und vor allem die Behandlung eines Infekts, im Idealfall vor Bildung eines Biofilms, stehen an oberster Stelle, eine Infektion des Knochens (Osteitis) zu verhindern. Die zunehmende Antibiotikaresistenz von SA und der Schutz durch den Biofilm legen nahe, die Forschung auf das Verhindern der Anheftung der Bakterien an Implantaten zu konzentrieren, so dass sich ein Biofilm nur stark reduziert oder gar nicht erst bilden kann. Implantate mit Antibiotikabeschichtung werden bereits verwendet, aber auf Grund der zunehmenden Resistenz von SA braucht es andere antimikrobiell wirksame Substanzen [19, 20]. Eine Alternative dazu könnte ein Bacteriocin namens Lysostaphin zu sein. Schon 1964 untersuchte Cropp [21] die Wirksamkeit von Lysostaphin an 252 SA-Stämmen aus Isolaten klinischer Herkunft. 1968 konnte Pulverer [22] an 230 SA-Stämme tierischer Herkunft die Wirksamkeit von Lysostaphin ebenfalls zeigen, wobei bei Pulverer nur 2 Stämme eine Resistenz gegenüber Lysostaphin aufwiesen und alle SA-Stämme bei Cropp sensibel gegenüber Lysostaphin waren.

Lysostaphin ist ein Zink-Ion Klasse III Bacteriocin [23], hergestellt von *Staphylococcus simulans* biovar *staphylolyticus* [24, 25], mit einem Molekulargewicht von 27 kDA [26] und 2 aktiven Domänen: einer N-terminalen katalytischen glycylglycin Endopeptidase als auch einer C-terminalen Zellwand gerichteten Domäne [27, 28], die das selektive Binden des Bacteriocins an der SA-Zellwand ermöglicht [29]. In der Zellwand bricht Lysostaphin die Pentaglycin-Brücke zwischen dem 3. und 4. Glycin durch Hydrolyse auf [27]. Ebenfalls ist Lysostaphin in der Lage, die Biofilm-Matrix zu zerstören und wirksam sowohl gegen Methicillin-sensible SA als auch gegen Methicillin-resistente SA zu sein [30–32], obwohl MSSA – Stämme einen *ica*-abhängigen und PIA-unterstützten Biofilm bilden und MRSA – Stämme mittels Fibronektin-bindender Proteine, Atl-unterstützter Zelllyse und eDNA an Oberflächen anheftet und einen PIA-unabhängigen Biofilm bilden [33].

In Tierversuchen konnte die Lysostaphin-Wirksamkeit ebenfalls *in vivo* gezeigt werden. In einem Kaninchenmodell mit Aortenklappen Endokarditis, ausgelöst durch einen MRSA, wurde Lysostaphin bis zu 3-mal täglich i.v. verabreicht, ohne dass sich bei den Tieren eine unerwünschte immunologische Reaktion auf das Lysostaphin zeigte [34]. In einem anderen Kaninchenmodell wurde die Hornhaut mit MRSA infiziert und mit Lysostaphin und / oder Vancomycin als Augentropfen behandelt. Hier zeigte sich eine Überlegenheit von Lysostaphin gegenüber Vancomycin [35]. In weiteren Untersuchungen von Lysostaphin als Nasensalbe bei nasaler MRSA- oder MSSA-Besiedelung an der Ratte, der i.v. Behandlung von MRSA bei systemischem Infekt und bei infiziertem Jugularvenenkatheter an der Maus zeigte sich ebenfalls die hohe Wirksamkeit von Lysostaphin, die sich in Kombination mit Nafcillin sogar noch steigern ließ [32, 36, 37]. Die Sensibilität von SA-Stämmen auf Lysostaphin liegt in einem hohen Glycin- und geringen Serin-Anteil in der Zellwand begründet. Obwohl SE sehr viel

weniger sensitiv auf Lysostaphin reagiert, kann dessen Biofilm durch Lysostaphin zerstört werden, allerdings nur bei sehr viel höherer Konzentration [38]. Im Gegensatz dazu zeigt Lysostaphin keine Wirkung auf den Biofilm des gram-negativen Bakteriums *Pseudomonas aeroguinosa* [38].

Zielsetzung

Auf Grund der großen Bedeutung von Knocheninfektionen (Osteitis) in der Unfallchirurgie, ausgelöst durch SA, war Ziel dieser Arbeit, ein kliniknahes, standardisiertes Implantat-assoziierten lokales Osteitis Mausmodell zu entwickeln, um im Anschluss daran, die Wirksamkeit von Lysostaphin-beschichteten Osteosynthese-Platten zur Verhinderung einer Osteitis zu testen.

Material und Methode

Alle hier beschriebenen Tierversuche wurden nach lokalen und nationalen ethischen Richtlinien und mit Genehmigung des Landesamtes für Natur, Umwelt und Verbraucherschutz Nordrhein-Westfalen durchgeführt (87-51.04.2010.A112).

Dieses Forschungsprojekt wurde finanziell unterstützt durch das „Zentrales Innovationsprogramm Mittelstand – ZIM“ des Bundesministeriums für Wirtschaft und Energie (KF2790101MK0), sowie der AO-Research Foundation (AO Start-Up grant S-11-34F).

Alle Experimente wie Operationen, radiologische und mikrobiologische Untersuchungen sowie funktionelle Tests wurden von mir durchgeführt.

Die Expertise der OP-Technik eignete ich mir in einem 2-tägigen Kurs der AO-Foundation an der Universität des Saarlandes an. Für die radiologischen Untersuchungen erwarb ich eine Fachkunde im Strahlenschutz durch die Tierärztekammer Nordrhein.

Für die OP-Assistenz, FACS und ELISA-Analysen standen mir Wei Meng (Publikation 1) und Christa Wilkens (Publikation 2) zur Seite. Die Plattenbeschichtungen mit

Lysostaphin und die Bestrahlungen mit 40 kGy wurden durch die Firmen Leukocare AG, München und BGS, Saale an der Donau durchgeführt.

Kumulativer Teil der Dissertation

Publikation 1: „Implant-Associated Localized Osteitis in Murine Femur Fracture by Biofilm Forming Staphylococcus aureus: A Novel Experimental Model“

Der erste Schritt der Forschungsarbeit bestand darin, ein standardisiertes Mausmodel mit einer akuten Implantat-assoziierten lokalen Osteitis zu entwickeln, welches die klinische Situation einer infizierten Osteosynthese mit einer akuten Osteitis am Patienten und der daraus resultierenden Frakturheilungsstörung widerspiegelt.

In Vorversuchen wurde bei 8 weiblichen BALB/c Mäusen, die sensitiv auf SA sind [39], der linke Femur mit einer MouseFix 4-Loch Osteosynthese-Platte fixiert, anschließend osteotomiert und mit unterschiedlichen mittleren colony forming units (CFU) von 10^3, 10^4 und 10^6 des MSSA-Stammes ATTC 29213 per Inokulation direkt an den Osteotomiespalt infiziert. Die Tiere wurden an Tag 7 und 14 standardisiert lavagiert und debridiert, wie es dem klinischen Standard bei Patienten mit Wundinfektionen entspricht. Die Frakturheilung wurde radiologisch kontrolliert. Die Lavagen und das Debridement dienten der Keimzahlreduktion, da es sonst zu einem fulminanten Infekt kommen kann. An Tag 28 wurden die Tiere nochmals final lavagiert / debridiert und geröntgt. Aus allen Lavagen wurden die CFUs bestimmt. Es zeigte sich, dass eine Infektion mit einer mittleren CFU von 10^3 ideal zur Induktion einer lokalen Osteitis war, eine höhere Keimzahl führte trotz Lavagen und Debridement frühzeitig zur Destruktion des Knochens.

Zur Etablierung des standardisierten lokalen Osteitis-Maus-Modells wurden vier verschiedene Mausgruppen mit drei unterschiedlich langen Beobachtungszeiträumen operiert (Tabelle 1), um die lokale und systemische Immunreaktion zu untersuchen.

Tabelle 1: Insgesamt wurden zur Modelletablierung 98 Tiere operiert. Die Kontrollgruppen umfassten Tiere, die nur SA an den Femur inokuliert bekamen, ohne Implantat und Osteotomie, sowie die Sham-OPs, bei denen die Mäuse nur das OP-Prozedere, ohne Infektion, Implantat und Osteotomie, durchlaufen haben. Demzufolge konnten Immunreaktionen, die allein auf Grund der OP bzw. der Keime auftraten, von den Immunreaktionen der Gruppen mit Osteotomie, Implantat und Infektion unterschieden werden.

	Anzahl der Tiere mit einem Beobachtungszeitraum von:		
Mausgruppe	**7 Tage**	**14 Tage**	**28 Tage**
nur SA Infektion	7	7	7
Sham-OP	7	7	7
keine Infektion, Osteotomie, Implantat	7	7	14
Infektion, Osteotomie, Implantat	7	7	14

Alle Tiere wurden an Tag 7, 14 und 28 (je nach Gruppe) lavagiert / debridiert und geröntgt. Aus den Lavagen wurden die CFUs sowie die Gesamt-Leukozytenzahl, PMNs und IL-6 bestimmt [40, 41]. Final wurde Herzblut mittels Punktion zur Bestimmung der Immunzellen gewonnen, außerdem wurden die rechten und linken Leisten-Lymphknoten entnommen und gewogen. Zur Beurteilung der Knochenbruchheilung wurde ein Punkte-Score entwickelt, bei dem für die Heilung des

Knochens 1 Punkt, für eine unveränderte Größe des Osteotomiespalts 2 Punkte und für die Vergrößerung des Spaltes oder Lyse des Knochens 3 Punkte vergeben wurden. Die sinkende Keimzahl in den Lavagen über die Zeit, die signifikant höhere Leukozyten-Anzahl, PMN- und IL-6 Menge in den Lavagen der infizierten Tiere gegenüber allen anderen Gruppen und die sehr geringen Konzentrationen der Immunzellen im Blut im Gegensatz zu den Lavagen, sowie die radiologisch ermittelte Knochenbruchheilung bei den nicht infizierten Tieren im Gegensatz zu den mit SA infizierten Mäusen (Abb. 1), ließ den Schluss zu, dass eine Inokulation von im Mittel 10^3 Keimen in Anwesenheit eines Implantates zu einer lokalen Osteitis bei der Maus führt, ohne dass diese zu einer Sepsis führt.

Abb. 1: Röntgenbild einer nicht infizierten Maus nach Osteotomie und Implantat mit vollständig konsolidierter Frakturzone (links) und einer infizierten Maus nach Osteotomie, Implantat und SA-Infektion mit einer Osteitis (rechts) 28 Tage post-operativ.

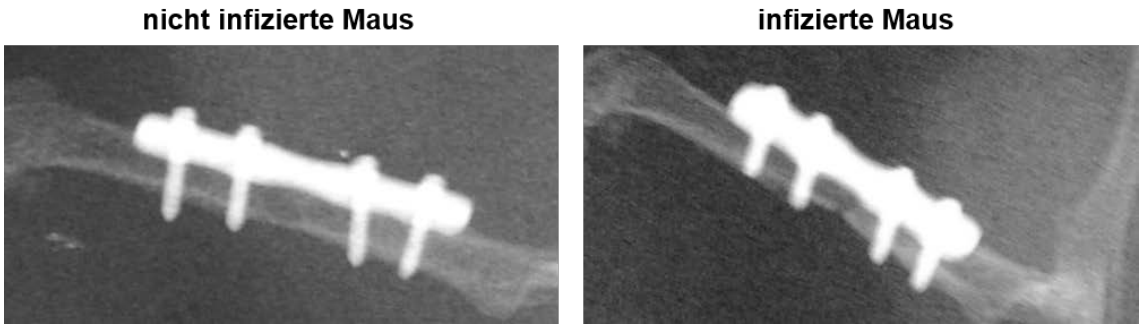

Des Weiteren zeigt dieses exemplarische Bild eines rechten und linken Leistenlymphknotens einer infizierten Maus ganz eindrucksvoll den lokalen Infekt (Abb. 2).

Abb. 2: Größenunterschied zwischen rechtem und linkem Leistenlymphknoten einer mit SA infizierten Maus mit Osteotomie und Implantat

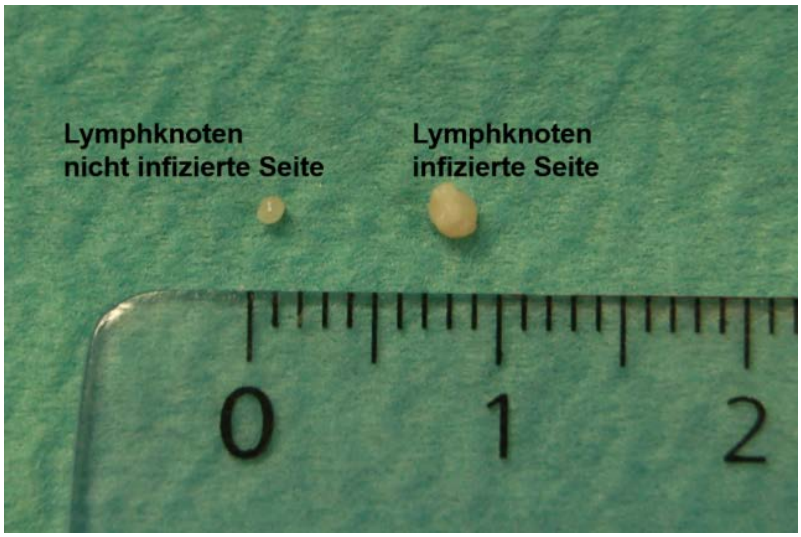

Zusammenfassend ist es gelungen, ein standardisiertes lokales Osteitis Mausmodell zu entwickeln, der die klinische Situation einer infizierten Fraktur abbildet. Im nächsten Schritt konnte nun die Wirksamkeit von Lysostaphin-beschichteten Implantaten untersucht werden.

Publikation 2: „Lysostaphin-Coated Titan-Implants Preventing Localized Osteitis by Staphylococcus aureus in a Mouse Model

Im zweiten Schritt der Forschungsarbeit wurde die Wirksamkeit von Lysostaphin-beschichteten Osteosynthese-Platten im zuvor etablierten Osteitis-Maus-Model untersucht.

Zunächst wurde zur Ermittlung der Mittleren Hemmkonzentration (MHK) von Lysostaphin eine Verdünnungsreihe von 0,01 µg/ml – 10 µg/ml hergestellt und mit einer auf McFarland (MF) 0,46 eingestellten SA-Kultur (ATTC 29213) inkubiert. Die MHK von Lysostaphin betrug 1 µg/ml.

Anschließend führte ich funktionelle Tests an Titanplättchen Grad 1 (Durchmesser 20 x 2 mm) durch, die mit verschiedenen Methoden und unterschiedlichen Lysostaphin-Konzentrationen durch die Firma Leukocare AG beschichtet worden waren. Letztendlich wurden die Plättchen mit 1 mg/ml Lysostaphin in einer poly(D,L)-laktid (PDLLA) Matrix und einer Schutzlösung (SPS, Leukocare AG, München) beschichtet. In den anschließenden *in vitro* Vorversuchen zeigte sich, dass Lysostaphin trotz der Prozedur der Beschichtung auf die Titanoberfläche seine Bioaktivität behielt. Von 42 Kulturen mit Lysostaphin-beschichteten Titanplättchen, die für 48 h mit dem SA-Stamm ATTC 29213 in Kultur gebracht und inkubiert wurden, zeigten nur 6 Kulturen Bakterienwachstum, alle anderen 36 Kulturen waren nach 48 h steril. Zur Sicherstellung einer ausreichenden Lysostaphin-Konzentration auf den kleinen MouseFix Osteosynthese-Platten (8 x 1 mm) wurden daraufhin insgesamt 10 Osteosynthese-Platten mit 1 mg/ml Lysostaphin beschichtet, 5 von diesen Osteosynthese-Platten wurden anschließend noch zusätzlich mit 40 kGy-β zu Sterilisationszwecken bestrahlt (Fa. BGS). Diese 10 Osteosynthese-Platten wurden in

eine Basiskultur mit einer CFU von 10^4 des SA-Stammes gebracht und für 48 h inkubiert. Auch hier zeigte nur jeweils eine Kultur Bakterienwachstum, alle anderen 8 Kulturen waren ebenfalls steril, so dass davon auszugehen war, dass die auf die MouseFix Osteosynthese-Platten gekoppelte Lysostaphin-Konzentration ausreichend war und die Bestrahlung der Osteosynthese-Platten ebenfalls keinen Einfluss auf die Bioaktivität von Lysostaphin hatte.

Zur Ermittlung der Wirksamkeit von Lysostaphin-beschichteten MouseFix Osteosynthese-Platten *in vivo* wurden 40 weibliche BALB/c Mäuse in 4 Gruppen (Tabelle 2) nach dem etablierten Osteitis Mausmodell operiert. Alle 40 Tiere wurden mit einer mittleren CFU von 10^3 mit dem SA-Stamm ATTC 29213 infiziert.

Tabelle 2: Zur Ermittlung der Wirksamkeit von Lysostaphin-beschichteten MouseFix-Osteosynthese-Platten wurden 4 Mausgruppen gebildet. Als Kontrolle dienten die Mausgruppen mit unbeschichteten Osteosynthese-Platten, sowie nur mit PDLLA-beschichtete Osteosynthese-Platten.

Mausgruppen	unbeschichtete Osteosynthese-Platten	PDLLA beschichtete Osteosynthese-Platten	Lysostaphin-beschichtete Osteosynthese-Platten	Lysostaphin-beschichtete Osteosynthese-Platten + 40 kGy-β
Anzahl	10	10	10	10

Die Tiere wurden gemäß dem etablierten Osteitis Mausmodell an Tag 7, 14 und 28 lavagiert / debridiert und geröntgt. Aus den Lavagen wurden die CFUs, die Gesamt-Leukozyten, PMNs und IL-6 bestimmt.

Der Punkte-Score zur Beurteilung der Knochenbruchheilung wurde von 3 Punkten auf 5 Punkte verfeinert, um eine klarere Abgrenzung zwischen Vergrößerung des Frakturspaltes, der Knochenlyse und der Knochendestruktion zu erhalten.

Schon an Tag 7 war in den Lavagen der Mausgruppen mit Lysostaphin-beschichteten Osteosynthese-Platten nur noch bei 3 von 20 Lavagen geringes Bakterienwachstum nachweisbar, die restlichen 17 Lavagen waren steril, im Gegensatz zu den beiden Kontrollgruppen, bei denen ohne Ausnahme eine CFU im Mittel von 10^4 in den Lavagen ermittelt werden konnte. Ebenso zeigte sich bei den Mausgruppen mit Lysostaphin-beschichteten Osteosynthese-Platten eine signifikant geringere Leukozyten-Anzahl, PMN und IL-6 Mengen in den Lavagen.

Die radiologische Analyse zeigte bei den Mausgruppen mit Lysostaphin-beschichteten Osteosynthese-Platten eine Konsolidierung der Frakturzone an Tag 28, wohingegen die Kontrollgruppen eine Osteitis entwickelten (Abb. 3).

Abb. 3: Repräsentative Röntgenbilder 28 Tage post-operativ der vier Mausgruppen. In der Mausgruppe ohne Plattenbeschichtung zeigt sich eine Lyse, in der PDLLA-Gruppe sogar eine Destruktion des Knochens, derweil es bei den beiden Gruppen mit Lysostaphin-beschichten Osteosynthese-Platten zu einer Ausheilung der Fraktur kam [42].

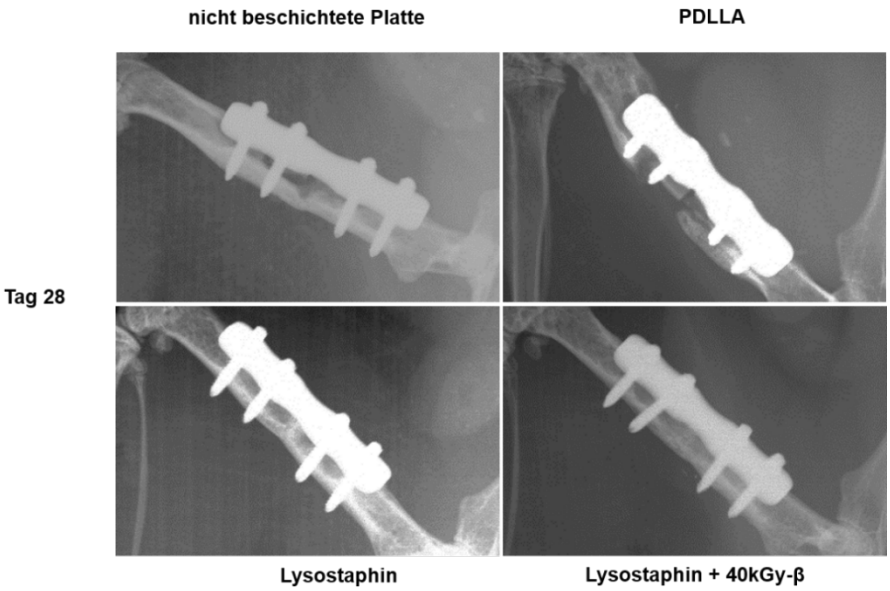

Im zweiten Schritt der Forschungsarbeit konnte die Wirksamkeit von Lysostaphin-beschichteten Osteosynthese-Platten in einem zuvor etablierten Osteitis-Maus Modell gezeigt werden.

Zusammenfassung

Die Implantat-assoziierte Osteitis, ausgelöst durch *Staphylococcus aureus* (SA), stellt heutzutage in der Unfallchirurgie und Orthopädie eine große Herausforderung dar. Bis zu 40 % der deutschen Bevölkerung sind Träger dieses Pathogens, der durch Frakturen mit Weichteilschaden oder bei Operationen in die Wunde gelangen kann. Dort besiedelt SA das Knochenimplantat, bildet einen Biofilm und schützt sich so vor Antibiotika, was oftmals zu einer Osteitis führt. In Zusammenspiel mit den aktivierten Immunzellen und ausgeschütteten Entzündungsfaktoren kommt es zu einer Zerstörung des Knochens und des umgebenden Gewebes. Somit repräsentiert das Beschichten von Implantaten mit Biofilm inhibierenden oder bakteriziden Substanzen einen neuen therapeutischen Ansatz.

Ziel dieser Promotionsarbeit war es, den Nutzen von Lysostaphin-beschichteten Implantaten hinsichtlich der Implantat-assoziierten Osteitis zu untersuchen.

Zunächst einmal wurde hierfür an BALB/c Mäusen ein standardisiertes Implantat-assoziiertes lokales Osteitis-Maus-Modell etabliert, bei dem die Tiere einen lokalen Infekt am Knochen ohne systemische Inflammation entwickelten. Den Tieren wurde der linke Femur osteotomiert, mit einer 4-Loch Osteosynthese-Platte stabilisiert und die Infektion erfolgte mit einer mittleren CFU von 10^3 des SA-Stammes ATTC29213 direkt an den Osteotomiespalt. Die Mäuse wurden an Tag 7, 14 und 28 lavagiert und debridiert, um aus den Lavagen die Keimzahl und die Immunzellen zu bestimmen. Die Frakturheilung wurde radiologisch mittels eines Punkte-Scores analysiert.

Anschließend wurde mittels des neu entwickelten und standardisierten Modells die Wirksamkeit von Lysostaphin-beschichteten Osteosynthese-Platten getestet. Es konnte gezeigt werden, dass Lysostaphin-beschichtete Osteosynthese-Platten in diesem standardisierten Osteitis-Maus-Modell eine lokale Osteitis verhindern können.

Die Beschichtung von Implantaten mit Lysostaphin stellt somit einen neuen therapeutischen Ansatz für Frakturen mit einem hohen Infektionsrisiko dar.

Summary

Implant-associated bone infection by *Staphylococcus aureus* (SA) is one of the major challenges in trauma and orthopaedic surgery today. Up to 40 % of the population in Germany is colonized by this pathogen. SA may penetrate wounds in open fractures or during extensive orthopaedic surgery. SA tend to attach on surface of implants and forms biofilm. Biofilm consists of an extracellular matrix, in which bacteria are embedded and protected from antibiotics and the immune response. This often results in an osteitis. Moreover, fracture healing is disturbed by activated immune cells and the inflammatory response. Thus, coating of implants with biofilm destroying or anti-microbial substances may represent a new therapeutic approach. The aim of this doctoral thesis was to evaluate the impact of Lysostaphin-coated implants for implant associated osteitis.

Firstly, a standardized implant-associated local fracture-osteitis mouse model without systemic inflammation was established. Here the left femur of BALB/c mice was osteotomized and a 4-hole plate was fixed to stabilize the femur. To induce an infection, SA-strain ATTC 29213 with an average CFU of 10^3 was inoculated directly into the fracture gap. Seven, 14 and 28 days after surgery lavage and debridement was performed. CFU and immune cells in lavage fluid were analysed. Score was developed to rate the fracture healing by radiographs. Inoculation of SA at a fracture site, which is stabilized with a plate results in a localized implant-associated osteitis with failure of fracture healing in this murine model.

Secondly, the potency of lysostaphin-coated implants was investigated. Using lysostaphin-coated plates for fracture stabilization prevented osteitis and enabled regular fracture healing. Thus, coating of implants with lysostaphin represents a novel therapeutic approach for fractures with a high risk for infection.

Ausblick

Die zunehmende Häufigkeit von Infektionen durch sogenannte Krankenhauskeime stellt nicht nur Ärzte sondern auch Forscher vor immer neue Herausforderungen. Die Einhaltung von Hygienevorschriften und die chirurgische Sanierung sind unerlässlich, aber die Resistenzsteigerung erfordert ein intensives Forschen in der zusätzlichen Bekämpfung von Infektionen in Form von neu entwickelten oder entdeckten Substanzen und deren klinischer Anwendbarkeit. Die hier vorgelegten Untersuchungen sollen ein erster Schritt hin zur klinischen Therapie sein. In den nächsten Jahren sind noch einige Fragen zu klären, z. B.: Was bewirken die Lysostaphin-beschichteten Platten in einem bereits länger bestehenden Infekt? Können diese dann noch eine Osteitis verhindern? Dazu ist ein Großtiermodell geplant, bei dem sich der Infekt erst eine Woche ausbreiten kann, um dann analog zum klinischen Vorgehen einen Plattenwechsel auf eine Lysostaphin-beschichtete Platte durchzuführen. Auch ist die Frage zu klären, inwieweit die PDLLA-Matrix der Beschichtung den Keimen eine zusätzliche Nische bietet, sich vor den Immunzellen und eventuell systemisch verabreichten Antibiotika zu schützen. Die Daten zeigen eine nicht signifikante aber trotzdem sichtbare Tendenz, dass Mäuse mit nur einer PDLLA-beschichteten Platte eine höhere Keimzahl in den Lavagen sowie eine stärkere Knochenzerstörung zeigten, als Tiere mit unbeschichteten Platten.

Darüber hinaus eignet sich dieses standardisierte Osteis-Maus-Modell für weitere Untersuchungen. So werden aktuell weitere Studien mit Antibiotika-angereichertem Knochenzement in einem Critical Size Defect und Untersuchungen zur Angiogenese durch Hyperbare Sauerstofftherapie durchgeführt.

Danksagung

Ganz herzlich möchte ich mich bei Prof. Klaus Pfeffer, Prof. Johannes Hegemann und Prof. Colin MacKenzie für wertvolle Ratschläge und ihre Unterstützung bedanken. Genauso herzlich bedanke ich mich bei Prof. Sascha Flohé und Prof. Tim Lögters für viele Stunden der Diskussion und den Freiraum, mich selbständig entwickeln zu können und nicht zu vergessen der Dank an das Laborteam für eine tolle Zeit.

Literatur

[1] **Campoccia D**, Montanaro L, Arciola CR (2006) The significance of infection related to orthopedic devices and issues of antibiotic resistance. Biomaterials 27(11): 2331–2339

[2] **An YH**, Friedman RJ (1998) Concise review of mechanisms of bacterial adhesion to biomaterial surfaces. J Biomed Mater Res 43(3): 338–348

[3] **Wright J**, Nair S (2010) Interaction of staphylococci with bone. Int J Med Microbiol 300(2-3): 193–204

[4] **Titécat M**, Senneville E, Wallet F et al. (2013) Bacterial epidemiology of osteoarticular infections in a referent center: 10-year study. Orthopaedics & Traumatology: Surgery & Research 99(6): 653–658

[5] **Robert Koch Institut** (2007) Prävention postoperativer Infektionen im Operationsgebiet: Empfehlung der Kommission für Krankenhaushygiene und Infektionsprävention beim Robert Koch-Institut (Prevention of postoperative surgical wound infection: recommendations of the Hospital Hygiene and Infection Prevention Committee of the Robert Koch Institute). Bundesgesundheitsblatt Gesundheitsforschung Gesundheitsschutz 50(3): 377–393

[6] **Kwok CS**, Crossman PT, Loizou CL (2014) Plate versus nail for distal tibial fractures: a systematic review and meta-analysis. J Orthop Trauma 28(9): 542–548

[7] **Götz F** (2002) Staphylococcus and biofilms. Mol Microbiol 43(6): 1367–1378

[8] **Schierholz JM**, Beuth J (2001) Implant infections: a haven for opportunistic bacteria. J Hosp Infect 49(2): 87–93

[9] **Robert Koch Institut** (2009) Staphylokokken-Erkrankungen, insbesondere Infektionen durch MRSA. https://www.rki.de/DE/Content/Infekt/EpidBull/Merkblaetter/Ratgeber_Staphylokokken_MRSA.html

[10] **Mah TF**, O'Toole GA (2001) Mechanisms of biofilm resistance to antimicrobial agents. Trends Microbiol 9(1): 34–39

[11] **Costerton JW**, Montanaro L, Arciola CR (2005) Biofilm in implant infections: its production and regulation. Int J Artif Organs 28(11): 1062-1068

[12] **Kirby AE**, Garner K, Levin BR (2012) The Relative Contributions of Physical Structure and Cell Density to the Antibiotic Susceptibility of Bacteria in Biofilms. Antimicrobial Agents and Chemotherapy 56(6): 2967–2975

[13] **Arciola CR**, Campoccia D, Speziale P et al. (2012) Biofilm formation in Staphylococcus implant infections. A review of molecular mechanisms and implications for biofilm-resistant materials. Biomaterials 33(26): 5967–5982

[14] **Yarwood JM** (2003) Quorum sensing in Staphylococcus infections. Journal of Clinical Investigation 112(11): 1620–1625

[15] **Gordon RJ**, Lowy FD (2008) Pathogenesis of Methicillin-Resistant Staphylococcus aureus Infection. CLIN INFECT DIS 46(S5): S350

[16] **Montanaro L**, Testoni F, Poggi A et al. (2011) Emerging pathogenetic mechanisms of the implant-related osteomyelitis by Staphylococcus aureus. Int J Artif Organs 34(9): 781–788

[17] **Wagner C**, Kondella K, Bernschneider T et al. (2003) Post-traumatic osteomyelitis: analysis of inflammatory cells recruited into the site of infection. Shock 20(6): 503–510

[18] **Wagner C**, Obst U, Hansch GM (2005) Implant-associated posttraumatic osteomyelitis: collateral damage by local host defense? Int J Artif Organs 28(11): 1172–1180

[19] **Campoccia D**, Montanaro L, Speziale P et al. (2010) Antibiotic-loaded biomaterials and the risks for the spread of antibiotic resistance following their prophylactic and therapeutic clinical use. Biomaterials 31(25): 6363–6377

[20] **Campoccia D**, Montanaro L, Arciola CR (2013) A review of the clinical implications of anti-infective biomaterials and infection-resistant surfaces. Biomaterials 34(33): 8018–8029

[21] **Cropp CB**, Harrison EF (1964) The in vitro effect of Lysostaphin on clinical iIsolates of *Staphylococcus aureus*. Can. J. Microbiol. 10(6): 823–828

[22] **Pulverer G** (1968) Untersuchungen mit Lysostaphin: II. Lysostaphin-Empfindlichkeit von 230 Staph. aureus-Stämmen tierischer Herkunkt. Z. med. Mikrobiol.u. Immunol.(154): 49–53

[23] **Bastos MdCF de**, Coutinho BG, Coelho MLV (2010) Lysostaphin: A Staphylococcal Bacteriolysin with Potential Clinical Applications. Pharmaceuticals 3(4): 1139–1161

[24] **Sloan GL**, Robinson JM, Kloos WE (1982) Identification of “Staphylococcus staphylolyticus” NRRL B-2628 as a Biovar of Staphylococcus simulans. International Journal of Systematic Bacteriology 32(2): 170–174

[25] **Recsei PA**, Gruss AD, Novick RP (1987) Cloning, sequence, and expression of the lysostaphin gene from Staphylococcus simulans. Proc Natl Acad Sci U S A 84(5): 1127–1131

[26] **Trayer HR**, Buckley, C E 3rd (1970) Molecular properties of lysostaphin, a bacteriolytic agent specific for Staphylococcus aureus. J Biol Chem 245(18): 4842–4846

[27] **Gargis SR**, Heath HE, LeBlanc PA et al. (2010) Inhibition of the activity of both domains of lysostaphin through peptidoglycan modification by the lysostaphin immunity protein. Appl Environ Microbiol 76(20): 6944–6946

[28] **Sabala I**, Jagielska E, Bardelang PT et al. (2014) Crystal structure of the antimicrobial peptidase lysostaphin from Staphylococcus simulans. FEBS J 281(18): 4112–4122

[29] **Gründling A**, Schneewind O (2006) Cross-Linked Peptidoglycan Mediates Lysostaphin Binding to the Cell Wall Envelope of Staphylococcus aureus. J. Bacteriol 188(7): 2463–2472

[30] **Dajcs JJ**, Thibodeaux BA, Hume EB et al. (2001) Lysostaphin is effective in treating methicillin-resistant Staphylococcus aureus endophthalmitis in the rabbit. Curr Eye Res 22(6): 451–457

[31] **Walencka E**, Sadowska B, Rozalska S et al. (2005) Lysostaphin as a potential therapeutic agent for staphylococcal biofilm eradication. Pol J Microbiol 54(3): 191–200

[32] **Kokai-Kun JF**, Chanturiya T, Mond JJ (2009) Lysostaphin eradicates established Staphylococcus aureus biofilms in jugular vein catheterized mice. Journal of Antimicrobial Chemotherapy 64(1): 94–100

[33] **McCarthy H**, Rudkin JK, Black NS et al. (2015) Methicillin resistance and the biofilm phenotype in Staphylococcus aureus. Front Cell Infect Microbiol 5: 1.

[34] **Climo MW**, Patron RL, Goldstein BP et al. (1998) Lysostaphin treatment of experimental methicillin-resistant Staphylococcus aureus aortic valve endocarditis. Antimicrob Agents Chemother 42(6): 1355–1360

[35] **Dajcs JJ**, Hume EB, Moreau JM et al. (2000) Lysostaphin treatment of methicillin-resistant Staphylococcus aureus keratitis in the rabbit. Invest Ophthalmol Vis Sci 41(6): 1432–1437

[36] **Kokai-Kun JF**, Walsh SM, Chanturiya T et al. (2003) Lysostaphin cream eradicates Staphylococcus aureus nasal colonization in a cotton rat model. Antimicrob Agents Chemother 47(5): 1589–1597

[37] **Kokai-Kun JF**, Chanturiya T, Mond JJ (2007) Lysostaphin as a treatment for systemic Staphylococcus aureus infection in a mouse model. Journal of Antimicrobial Chemotherapy 60(5): 1051–1059

[38] **Wu JA**, Kusuma C, Mond JJ et al. (2003) Lysostaphin disrupts Staphylococcus aureus and Staphylococcus epidermidis biofilms on artificial surfaces. Antimicrob Agents Chemother 47(11): 3407–3414

[39] **Köckritz-Blickwede M von**, Rohde M, Oehmcke S et al. (2008) Immunological Mechanisms Underlying the Genetic Predisposition to Severe Staphylococcus aureus Infection in the Mouse Model. The American Journal of Pathology 173(6): 1657–1668

[40] **Yoshii T**, Magara S, Miyai D et al. (2002) Local levels of interleukin-1beta, -4, -6 and tumor necrosis factor alpha in an experimental model of murine osteomyelitis due to staphylococcus aureus. Cytokine 19(2): 59–65

[41] **Prabhakara R**, Harro JM, Leid JG et al. (2011) Murine Immune Response to a Chronic Staphylococcus aureus Biofilm Infection. Infection and Immunity 79(4): 1789–1796

[42] **Windolf CD**, Lögters T, Scholz M et al. (2014) Lysostaphin-coated titan-implants preventing localized osteitis by Staphylococcus aureus in a mouse model. PLoS ONE 9(12): e115940

Anhang

Implant-Associated Localized Osteitis in Murine Femur Fracture by Biofilm Forming *Staphylococcus aureus*: A Novel Experimental Model

Ceylan D. Windolf,[1] Wei Meng,[1] Tim T. Lögters,[1] Colin R. MacKenzie,[2] Joachim Windolf,[1] Sascha Flohé[1]

[1]Department of Trauma- and Hand Surgery, Heinrich-Heine University Duesseldorf, Moorenstr. 5, 40225, Duesseldorf, Germany, [2]Institute of Medical Microbiology and Hospital Hygiene, Heinrich-Heine University, Duesseldorf, Germany

Received 2 March 2013; accepted 26 June 2013
Published online in Wiley Online Library (wileyonlinelibrary.com). DOI 10.1002/jor.22446

ABSTRACT: *Staphylococcus aureus* (SA) is the most common causative agent for implant-associated osteitis. The present study characterizes a novel model of a low grade acute SA osteitis with bone defect in the femur which is stabilized by a titanium locking plate. Wild-type Balb/c mice were osteotomized, fixed by a locking plate and infected with SA. Mice underwent debridement 7 and 14 days later and were sacrificed at Day 28. At Days 7, 14, and 28 after inoculation local and systemic cell populations and IL-6 were analyzed. Fracture healing was quantified by radiography. The control group underwent the same procedure without infection. The bacterial load of implant-associated osteitis with biofilm formation was quantified by counting CFU and real-time PCR. Fracture healing determined by radiography was delayed in infected compared to non-infected mice. Throughout the investigation period CFU and leukocyte counts, as well as IL-6 levels were found to be significantly elevated in infected mice at the infection site but not systemically. Our murine model allows the detailed investigation of implant associated localized osteitis with biofilm producing SA and its influence on fracture healing. The model provides a tool to analyze therapeutic or prophylactic approaches to the problem of biofilm-associated osteitis. © 2013 Orthopaedic Research Society Published by Wiley Periodicals, Inc. J Orthop Res

Keywords: mouse; infection; osteitis, biofilm, *Staphylococcus aureus*

Infection in implants has emerged as one of the major challenges in trauma and orthopedic surgery today. The skin and various mucosal barriers are host to opportunistic pathogens like *Staphylococcus epidermidis* and *Staphylococcus aureus* (SA).[1,2] 20% of the US population shows a chronic and at least another 30% a temporary skin colonization of SA.[3] Extensive orthopedic surgery or fractures accompanied by severe tissue injury are associated with an impaired local immune response and thus are at risk for implant-associated infections by opportunistic pathogens. Two-thirds of implant-associated infections are caused by staphylococci, SA (34%) and *S. epidermidis* (32%).[4,5] Microorganisms penetrate the wound and subsequently attach to the surface of implants and also especially devitalized bone. Bacteria adhere to the foreign body surface and form a hydrated matrix of extracellular components defined as a biofilm.[1] The biofilm represents a multilayer cell cluster of sessile bacteria, which produce, and are embedded in, the extracellular substance including several proteins.[1,2,6] Biofilm formation represents the prevalent source of bacterial growth on implants and origin for chronic osteitis.[7,8] The biofilm consists of bacteria (1) in their dividing planktonic form which are potentially susceptible to antibiotics and (2) predominantly in their sessile form, which have a reduced metabolic and replication rate and are thus far less susceptible to antibiotics.[9] Furthermore the biofilm matrix itself provides a barrier between bacteria and the innate or adaptive immune response and antibiotics.[10,11] Thus, almost all implant associated infections generated by biofilm producing bacteria result in a subacute to chronic osteitis with progressive bone destruction and subsequent delayed healing.[12]

Treatment options of osteitis biofilm associated with SA are limited. Local surgical debridement, lavage procedure, and the application of antibiotics represent the first therapeutic options for infected osteosynthesis. However, these procedures are frequently ineffective and only successful in case of early diagnosis. Once established, foreign body infections caused by biofilms are very unlikely to be resolved by either antibiotic therapy, local surgical debridement, or the host immune system. Removal of the foreign material and thus the basis for the biofilm remains the only therapeutic option. The consequences of removing prostheses and internal fixation devices are grave and thus every effort is made to prevent this. Thus, the development of therapeutic strategies aimed at biofilms is a major challenge for orthopedic trauma research. A limited number of animal models with an infected implant by a biofilm forming bacteria exist for this purpose and a murine model that combines an implant-associated osteitis with a standardized fracture at the infection site, thus mimicking the clinical situation in humans is not available at all. The aim of this study was to establish and characterize a mouse model of an acute implant-associated osteitis with biofilm-forming bacteria which simulates the clinical situation of an infected osteosynthesis with acute osteitis and non-union of the fracture. The present study describes a novel model of a low grade acute SA osteitis with a bone defect in the femur stabilized by a titanium locking plate.

Grant sponsor: Zentrales Innnovationsprogramm Mittelstand (German ministry of economics and technology); Grant sponsor: AO-Research Foundation.
Correspondence to: Ceylan D. Windolf (T: +49-211-302039-232, F: +49-211-302039-248; E-mail: ceylan.windolf@uni-duesseldorf.de)

METHODS

Animals

Ten to 12-week-old female wild-type Balb/c mice weighing up to 21 g (animal facility of the Heinrich-Heine-University Duesseldorf; Tierversuchsanlage, TVA, Germany), were used for the experiments. Balb/c mice are highly susceptible for SA infections in contrast to other mouse strains.[13] All animal procedures were carried out under local and national ethical guidelines and were approved by the regional ethical committee, Regional Office for Nature, Environment and Consumer Protection Nordrhein-Westfalen, Germany, with the ethical approval ID 87-51.04.2010.A112.

Low Grade Acute Osteitis Model

Our acute osteitis fracture model represents a modification of a fracture model of mouse femur described by Holstein et al.[14] followed by inoculation of the fracture site with a defined amount of SA. All operations were performed in an aseptic operating room of our local animal facility. In detail mice were anesthetized by i.p. injection of xylazine (25 mg/kg body weight) and ketamine (75 mg/kg body weight). The thigh was gently shaved and cleaned with betadine and alcohol swabs. After skin incision under sterile conditions, the fascia was opened, and the plate was fixed (MouseFix plate by RISystem, Davos, Switzerland). An osteotomy using a Gigly saw (diam. 0.22 mm, RISystem) was performed in midshaft of the femur to create a bone defect. Afterwards 1 μl of a standard quantity of SA strain ATCC 29213 in phosphate buffered BactoTryptic Soy Broth was inoculated with a micropipette into the fracture gap. In order to mimic the clinical situation of an infected osteosynthesis mice were anesthetized again 7 and 14 days after primary surgery and a wash-out (lavage) with debridement (excision) of infected tissue was performed. For the lavage the thigh was reopened under sterile conditions. The exposed soft tissue was irrigated twice with 250 μl PBS. The lavage fluid was recovered and PBS added to a total volume of 1 ml. Local debridement consisted of removal of devascularized and fibrous tissue with a surgical spoon without involving periost. All surgical interventions were made by the same surgeon. The intention of these procedures was to mimic the surgical therapy of an infected implant in clinical routine. In addition, the lavages offer the possibility to collect samples from the local site of infection and to perform therapeutic intervention in this model. At Day 28 animals were sacrificed, blood was collected by cardiac puncture and lavage of the femur was performed again. Femora were resected and the plates removed for biofilm detection and histological evaluation (see below). Mice were classified into three groups: (1) Plate fixation, osteotomy and inoculation of SA (infected mice; $n = 28$); (2) Plate fixation and osteotomy without infection (non-infected mice; $n = 28$); (3) Sham ($n = 14$). The sham group underwent skin incision and exposure of the femur.

S. aureus Strain ATCC 29213

SA strain ATCC 29213 was cultivated overnight in Bacto-Tryptic Soy Broth, adjusted to McFarland 1, and then diluted 1: 10,000, 1:1,000, 1:100, and 1:10. Thereafter 10 μl of each suspension were plated on Columbia-Agar + 5% sheep-blood (bioMérieux, Nürtingen, Germany) and cultivated overnight at 37°C in normal atmosphere. After overnight culture the CFU were determined. For each dilution the CFU was determined four times and the average CFU were 2.00E+03 for 1:10,000, 5.00E+04 for 1:1,000, 1.00E+06 for 1:100, and 5.00E+06 for 1:10.

Radiographic Analysis

At Days 0, 7, 14, and 28 after plate fixation anteroposterior radiographs (40 kV, 16 mA) of the femora were performed under anesthesia. In order to define the fracture healing on radiographs we developed a score to evaluate the fracture gap size. The titanium 4-hole MouseFix plate has a length of 8 mm. Measuring the size of the whole plate on the image allowed calculation of a factor for each individual radiograph and subsequently a standardized estimation of the fracture gap. Decreasing fracture gaps representing fracture healing were rated with 1 point; constant fracture gaps, meaning non-union, were allocated 2 points while increasing fracture gaps indicating osteolysis were allocated 3 points.

Counts of Colony-Forming Units (CFU)

The number of colony-forming units (CFU) was determined in the lavage and blood at defined time points. Bacteria from the thigh were obtained by lavage under aseptic conditions. Blood was obtained by cardiac puncture. Subsequently, 200 μl of blood and lavage were serially diluted in PBS and four replicates of 10 μl of each dilution plated on Columbia Agar plates with 5% sheep blood and incubated under aerobic conditions at 37°C. Bacterial colonies were counted after 24 h. Results were specified as CFU per 1 ml.

Evaluation of Local IMMUNE Response

The local inflammatory response was characterized by measuring the cellular components in the lavage and in sera using flow cytometry (FACSCanto II; BD Biosciences, Heidelberg, Germany). For cell typing, forward and side scatter characteristics and the following antibodies were used for myeloid cells (BD Pharmingen, Frankfurt Germany: APC Rat Anti-Mouse CD11b), PMN (FITC Rat Anti-Mouse Ly-6G; BD Pharmingen), monocytes (Anti-Mouse Ly-6C PerCP-Cy5.5; eBioscience, Frankfurt, Germany), T-cells (APC-Cy7 Rat Anti-Mouse CD3 Molecular Complex; BD Pharmingen) and B-cells (PE-Cy7 Rat Anti-Mouse CD19; BD Pharmingen).

Quantification of Interleukin (IL)-6 by ELISA

IL-6 levels in the lavage and sera were determined using a commercially available IL-6 ELISA kit according to the manufacturer's instructions (R&D Systems, Abingdon, UK). The lower detection limit for IL-6 was 16 pg/ml.

Histology and Scanning Electron Microscopy

Bones for histology were fixed in 4% buffered formalin for 1 day and then decalcified for 12 days. The decalcified bones were embedded in paraffin according to standard procedures. Sections (2 μm) were stained with hematoxylin and eosin (HE). In addition Giemsa staining of bone specimens in infected groups was performed for specific detection and quantification of bacteria. The callus formation was messured with AxioVision SE64 Rel. 4.9 (Zeiss, Jena, Germany).

Scanning electron micrographs (JEOL JSM-35CF Scanning Microscope, Eching, Germany) of titanium discs and removed plates with infected bone was performed. Before EM, plates attached to the bone were removed, dehydrated in an acetone series and freeze-dried with liquid CO_2 (Leica EM CPDO 30, Wetzlar, Germany).

Biofilm Generation and Quantification in vitro

The SA strain ATCC 29213 was cultivated in BactoTryptic Soy Broth overnight. In order to form a biofilm, the overnight culture was diluted 1:100 and the titanium discs Grade 1 (ARA-T Advance GmbH, Dinslaken, Germany) with diameter of 20 mm × 2 mm were placed in the bacterial culture and

incubated for 48 h at 37°C and 100 rpm. Thereafter the titanium discs were gently washed with PBS three times to remove planktonic cells. The discs were then sonicated (B. Braun Labsonic, output power 550 W) for 3 min at half power and again gently washed again three times.[15] To quantitate the bacteria in the biofilm removed by sonication, the suspension and the remaining bacteria on the titanium discs were lysed with MRSA-lysis-buffer (EDTA, Tween 20, Triton X-100, Tris/HCl; Sigma–Aldrich, Hamburg, Germany) to gain the DNA. A SA specific *nuc*-Gen real-time PCR was used to quantitate the bacteria (Biorad CFX 96; Primer: Oligo nuc-for, nuc-rev, nuc-Probe from Metabion, Martinsried, Germany; Mastermix Black Hole Quencher 5′-Fam-3′-BHQ-1 from Qiagen, Hilden, Germany).[16,17] In order to quantify the *nuc*-Gen a standard was produced by cloning the target *nuc*-gene in the TOPO vector as described in the manufacturer's instructions (Kit Macherey-Nagel (MN) NucleoSpin® Extract II Nucleic Acis and Protein Purification, TOPO® Cloning, Reaction + Transformation, continued). The plasmid was then purified (High Pure Plasmid Isolation Kit from Roche, Grenzach-Wyhlen, Germany), quantified and diluted to *nuc*-standards with 10E+09, 10E+07, 10E+05, 10E+03, and 10E+02 plasmid copies/μl.

Statistical Methods

All data are expressed as median and 5 and 95 percentile or mean and standard error as indicated in the figure legends. Data were tested for statistical significance with two-tailed Mann–Whitney-test using GraphPad Prism5 (GraphPad Software, San Diego, CA): p values ≤ 0.05 were considered as significant.

RESULTS

Localized Implant Associated Acute Osteitis

At first we determined the amount of methicillin-sensitive SA strain ATCC 29213 which induces a localized, low grade acute osteitis. Bacteria in between 2.00E+03 and 5.00E+06 bacteria/mouse, in 1 μl PBS were applied directly into the fracture gap as illustrated in Figure 1. To determine the optimal infection dose in order to cause an acute osteitis that remained localized, bacteria in counts from 10E+03 to 10E+06 were applied directly to the fracture gap in 1 μl PBS.

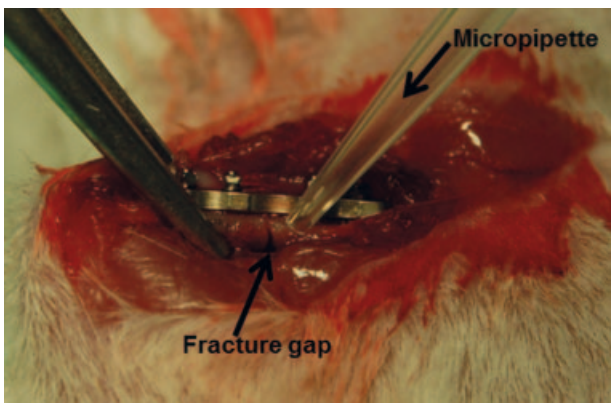

Figure 1. Demonstration of implant-associated fracture-osteitis model. Intraoperative picture showing stable fixation of a femur osteotomy by a locking plate (MouseFix plate, AO-Foundation, Research Implants Systems, Davos, Switzerland) and inoculation of *Staphylococcus aureus* (CFU ± 2 × 10E+03) into the fracture gap with a micropipette.

It was found that the application of SA at an infection dose of 10E+06 resulted in a complete destruction of the femur with plate loosening and dislocation as well as severe clinical signs of the systemic infection. Based on these findings we choose a bacterial load of 10E+03 SA/mouse for all further experiments to cause an acute but localized osteitis based on primary low grade infection.

Absence of Fracture Healing in Infected Mice

A bacterial inoculation of 10E+03 resulted in a low grade acute osteitis despite two lavage procedures at Days 7 and 14 after fracture. Radiographs of all femora from non-infected mice showed early fracture healing by Day 7 and complete fracture consolidation by Day 28. In contrast all femora of mice infected by SA showed no fracture healing at any time point. Furthermore, for all cases osteolysis was present and the fracture gap was increased (Fig. 2). The fracture gap was evaluated using a semi quantitative score as indicated above. Infected mice displayed a significantly reduced bony healing 7 ($p = 0.0208$); 14 ($p = 0.0218$); and 28 days ($p = 0.0349$) after surgery as indicated by the higher scores at the corresponding time points compared to control animals (Fig. 3). This result also was affirmed histological by analyzing the callus formation (data not shown).

Bacterial Growth in Bone, Soft Tissue, and Implant in Infected Mice

To provide evidence for implant associated local acute osteitis the number of CFU in lavage, blood, and bone were determined. No bacteria were detected in blood

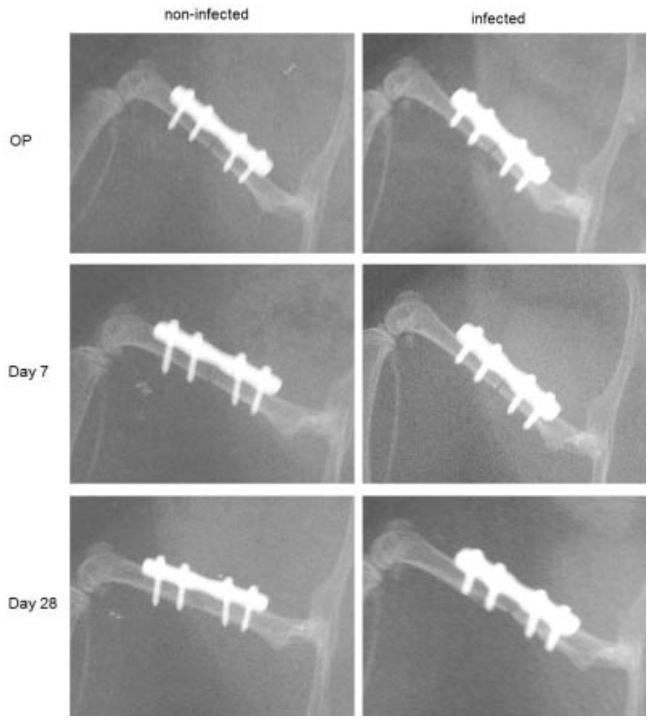

Figure 2. Radiographic augmentation of fracture gap size and osteolysis around osteotomy of infected mice versus non-infected mice at Days 0, 7, and 28 after osteotomy and plate fixation.

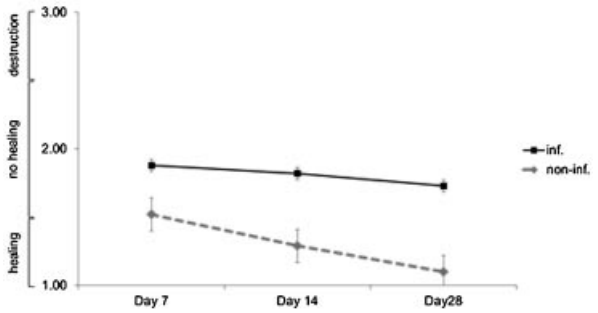

Figure 3. Absence of fracture healing and osteolysis of femora of infected mice. Standardized radiographic quantification of fracture healing from non-infected ($n = 47$) and infected ($n = 53$) mice at Days 7, 14, and 28 after osteotomy and fracture fixation. Infected mice showed significant difference in fracture gap size at Day 7 ($p = 0.0208$), Day 14 ($p = 0.0218$), and Day 28 ($p = 0.0349$). Data are expressed as mean and standard error.

at any time point. CFU counts were measured in the lavage at Days 7, 14, and 28 after primary surgery in infected mice, as shown in Figure 4A. There was a tendency towards lower, non-significant bacterial load after 28 days indicating the establishment of acute persisting infection. In the uninfected controls minor bacterial growth could be detected at Day 7. This is most likely explained by a contamination during the initial surgical procedure which resolved over time. No bacterial growth was also found in sham-operated mice at any time point.

Giemsa staining of bony specimens collected 28 days after fracture and SA inoculation demonstrated the presence of bacteria within the bone adjacent to the drill holes (Fig. 4B). This finding was also confirmed by the positive cultures of homogenized bone specimens collected after surgery in the infected mice. Bone specimens collected from the control group were negative for bacterial growth.

Cellular Immune Response in Acute Osteitis

Macroscopically, on Days 7, 14, and 28, all mice of the infection group demonstrated a localized infection of the left thigh with an increased amount of semiliquid, fibrin like tissue which coated the bone and the plate. During debridement at Days 7, 14, and 28, all infected tissue was excised and the surgical field was irrigated with PBS. In order to evaluate the local immune response the cellular composition of the lavage was determined. The number of leukocytes in the lavage of infected mice was significantly increased on Days 7 (15 859/ml), 14 (1576/ml), and 28 (560/ml) after internal fixation compared to control group median (154/ml after 7 days, 16/ml after 14 days, and 0/ml after 28 days; Fig. 5A). The predominant cells in the lavage of infected mice after the first week were neutrophils and only a minimal number of antigen presenting cells such as monocytes. The relative cellular distribution revealed more monocytes and fewer neutrophils compared from Days 7 to 14 (Fig. 5B). B and T cells were found in the lavage only in minimal numbers at all-time points (data not shown). Leukocyte counts in the blood of infected mice were significantly elevated only on Day 14 in the infected mice. All other groups and time points remained within normal range (data not shown).

Non-Cellular Immune Response in Acute Osteitis

The concentration of IL-6 was significantly increased in the lavage fluid of infected mice compared to non-infected mice on Days 7 ($p < 0.0001$) and 14 ($p = 0.0004$; Fig. 6). In contrast to this, only minimal IL-6 concentrations were only found in blood of infected mice after 7 and 14 days (data not shown).

S. aureus Infection With Biofilm Formation In Vitro and In Vivo

The suspension after sonication was examined for bacteria and showed a median $1.8 \times 10E{+}04$ CFU ($n = 50$), which demonstrates the presence of bacteria firmly attached to the titanium plates. Furthermore this was confirmed by real time PCR of the SA using the specific single copy *nuc*-gen as a target sequence.

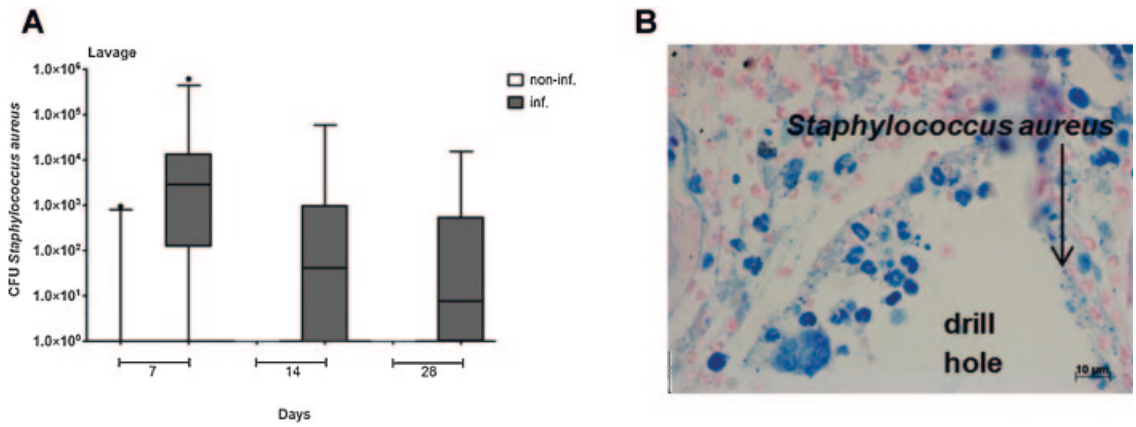

Figure 4. (A) Local detection of *Staphylococcus aureus* around the fracture site of non-infected ($n = 47$) and infected ($n = 53$) mice at all time points with decreasing count from Days 7 to 28 ($p = 0.0262$). Data are expressed as median and 5 and 95 percentile, dots are outliers. (B) Intraosseous detection of *Staphylococcus aureus*. Representative Giemsa stained section from a decalcified femur showing *Staphylococcus aureus* adjacent to the drill holes of the plate screws.

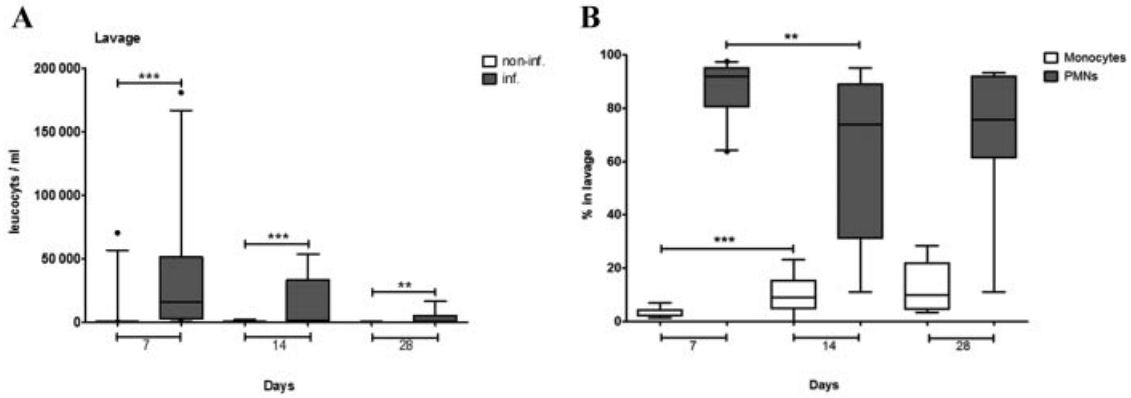

Figure 5. (A) Enhanced leukocyte recruitment to infection site. Leukocyte counts in the lavage of mice at Days 7–28 in non-infected ($n = 47$) and infected mice ($n = 53$). Differences were significant at all-time points (7 days: $p < 0.0001$; 14 days: $p = 0.0004$; 28 days: $p = 0.0048$). Data are expressed as median and 5 and 95 percentile, dots are outliers. (B) Relative increased neutrophils at infection site in low grade acute osteitis. Percentage distribution of monocytes and neutrophils in lavage fluid of infected mice on Days 7, 14, and 28 after fracture with ($n = 53$). $^{**}p = 0.0019$, $^{***}p = 0.0005$. Data are expressed as median and 5 and 95 percentile.

Real time PCR revealed an even higher number of bacteria (median 2.6 × 10E+05) in the sonicated suspension. However, even sonication as described before did not result in a complete separation of all adherent biofilm-embedded staphylococci from the discs. DNA-extraction with MRSA-lysis-buffer and *nuc*-gen specific real time PCR revealed the presence of approximately 3.6 × 10E+04 bacteria on the discs even after sonication (Fig. 7). Both the results of CFU and PCR demonstrate that the applied SA strain ATCC 29213 is a potent producer of biofilm. To further demonstrate the presence of biofilm we performed scanning electron microscopy (SEM) of the titanium discs incubated with SA. As illustrated in Figure 8A, biofilm formation with embedded staphylococci was detectable on the titanium discs. In order to confirm our results in vivo MouseFix plates of infected mice were removed at day 28 after surgery. A macroscopically matrix could be demonstrated on the surface of the plates containing embedded bacteria and host leukocytes (Fig. 8C). In accordance with this the presence of sessile bacteria was also confirmed in vivo by a PCR and bacterial CFU of MouseFix plates removed at Day 28 after surgery. Sonication of the in vivo infected MouseFix plates revealed a lower number of bacteria recovered by sonication of the implant in the *nuc*-gen PCR in comparison to conventional CFU.

DISCUSSION

The present study characterizes a murine model of a combination of low grade acute osteitis and fracture, which simulates key aspects of the pathogenesis and therapy of an implant associated osteitis: Firstly, it addresses qualitative and quantitative aspects of biofilm formation on metal surfaces and secondly, it deals with the potential interaction of bone healing and infection. In this respect we were able to demonstrate and document a significant delay in bone healing in

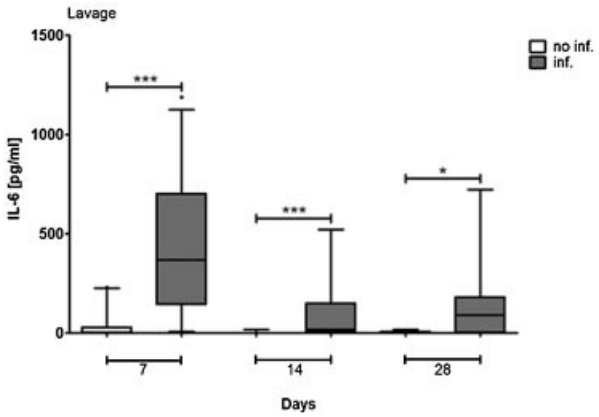

Figure 6. IL-6 levels are raised locally but not systemically in early phase of infection. IL-6 was measured in lavage fluid as described in the methods on Days 7, 14, and 28 (non-infected: $n = 47$; infected: $n = 53$) after fracture without and with bacterial infection. $^{*}p < 0.05$, $^{***}p < 0.001$. Data are expressed as median and 5 and 95 percentile, dots are outliers.

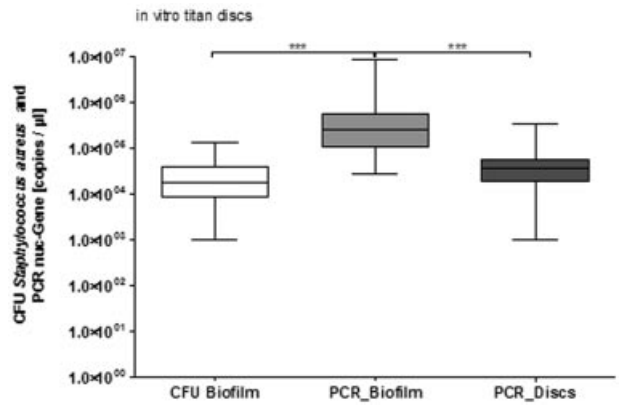

Figure 7. Quantification of biofilm formatting *Staphylococcus aureus* in vitro. Bacterial colony forming units (CFU) measured from sonicated suspensions. Real time PCR of the *Staphylococcus aureus* was performed from sonicated suspension and from titanium discs. Data are expressed as median and 5 and 95 percentile.

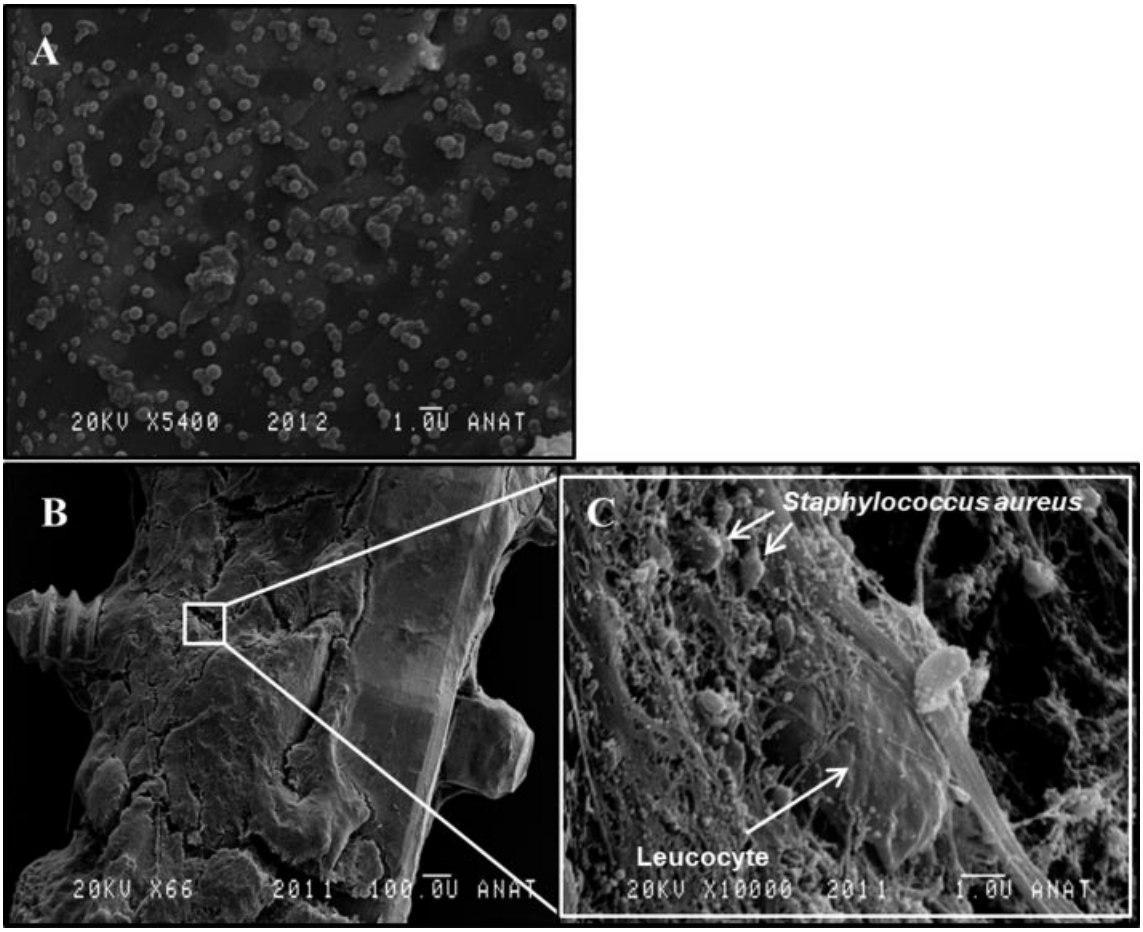

Figure 8. Qualitative evidence of biofilm in vitro and in vivo. Electron microscopic microphotograph showing *Staphylococcus aureus* embedded in biofilm on a titanium disc in vitro (A), and on a MouseFix plate and bone in vivo (B, two magnifications 66× and 10,000×). Plate and femur were removed from the mouse at Day 28 after osteotomy, plate fixation and inoculation of *Staphylococcus aureus*.

infected animals. Thirdly, this model includes therapeutic interventions in terms of staged lavages, an intervention simulating a therapeutic algorithm of early implant-associated infections. In addition the model offers the possibility to examine the local environment of the infected bone in terms of microbiological, immunological, and osteological aspects. Finally the staged lavages also provide an opportunity to test specific therapeutic strategies aimed at biofilm-associated osteitis. Restrictively we had to mention a limitation of that study. Fracture healing only was determined semi quantitatively by X-rays and resultant bony healing score. Micro-CT would have been preferable but was not available.

There are a variety of mouse or rat models of chronic bone infection, none of which combines all the above-mentioned aspects. Most animal models induce a chronic bone infection by bacterial inoculation into the medullary cavity with or without an additional foreign body, for example a nail or k-wire[17,18] loaded with defined bacterial cultures inserted into the bone.[19] All these models induce a constant bone infection with bacterial growth in the medullary cavity. Likewise bacteria have been demonstrated in the medullary cavity and the cortex in our model which defines the diagnosis of an osteitis. However, most murine osteitis models do not include a fracture into their experimental protocol. Our model offers the opportunity to investigate the interaction between the infection and the process of fracture healing in detail. A comparable model was introduced by Chen et al.[20] in which a mid-diaphyseal defect on rat femur was introduced, stabilized with a polyacetyl plate and Kirschner wires, and thereafter a chronic bone infection caused by application of bacteria-containing collagen fleece into the osteotomy. Although Chen et al. clearly demonstrated a chronic bone infection by both bacterial cultures of bone specimens and histology, a detailed analysis substantiating the presence of a biofilm was not performed. Apart from the fracture simulation, the type of stabilization is of particular relevance for fracture healing as well as the infection process. In our model a titanium plate with interlocking screws was used. Application of a plate with interlocking screws results in a high fracture stability ensuring a reliable fracture healing in mice.[14,21,22] In

particular this stable fracture fixation provides the opportunity to investigate the influence of an implant-associated infection of a primary stable osteosynthesis on fracture healing. A direct contamination of the plate with a defined bacteria count in vivo, without application of foreign carrier matrix such as bovine collagen, represents the clinical scenario. Furthermore, it has been shown that carrier matrices themselves can induce a relevant immune reaction.[23]

Mechanisms underlining bacterial induced inflammation in bone tissue are poorly understood. A number of cytokines play a relevant role in the pathogenesis of osteitis. There is strong evidence that these cytokines are induced by staphylococcal infection of the bone and contribute to infection-related bone destruction. In patients with osteitis plasma levels of TNFα, IL-1β, and IL-6 are elevated.[24,25] While TNFα and IL-1β most likely originate from infiltrating immune cells in bone infection, IL-6 is produced by osteoblasts itself in response to a variety of bacteria including SA.[26] IL-6 increases bone resorption and stimulates osteoclast differentiation in the presence of osteoblasts.[27] We could observe elevated IL-6 levels in the lavage of the infected bone in our model particularly in the earlier phase of infection. The enhanced local levels of IL-6 in the infected mice correlate with the absent fracture healing and formation of osteolysis at these time points. In summary, this murine model of a low grade acute, localized, implant-associated osteitis resembles the clinical setting of an infected osteosynthesis in terms of failure of fracture healing, acute localized osteitis with no bacterial dissemination and proven biofilm formation, typical pattern of a persistent immune response in terms. Furthermore the model provides a useful method of investigating the immune reaction to this common disease and the effect of therapeutic interventions such as staged lavages. The model also provides an opportunity to evaluate other innovative therapeutic strategies such as biofilm-preventative antimicrobial implant coatings or local immunostimulatory strategies.

ACKNOWLEDGMENTS

We thank K. Pfeffer, J. Hegemann, M. Sager, N. Stoecklein for valuable advice and friendly provision of experimental facilities, K. Zanger for electron scanner micrograph.

REFERENCES

1. Götz F. 2002. Staphylococcus and biofilms. Mol Microbiol 43:1367–1378.
2. Schierholz JM, Beuth J. 2001. Implant infections: a haven for opportunistic bacteria. J Hosp Infect 49:87–93.
3. Gordon RJ, Lowy FD. 2008. Pathogenesis of methicillin, resistant *Staphylococcus aureus* infection. Clin Infect Dis 46:350–359.
4. Campoccia D, Montanaro L, Arciola CR. 2006. The significance of infection related to orthopedic devices and issues of antibiotic resistance. Biomaterials 27:2331–2339.
5. Wright J, Nair S. 2010. Interaction of staphylococci with bone. Int J Med Microbiol 300:193–204.
6. Yarwood JM. 2003. Quorum sensing in Staphylococcus infections. J Clin Invest 112:1620–1625.
7. An YH, Friedman RJ. 1998. Concise review of mechanisms of bacterial adhesion to biomaterial surfaces. J Biomed Mater Res 43:338–348.
8. Hudson MC, Ramp WK, Frankenburg KP. 1999. *Staphylococcus aureus* adhesion to bone matrix and bone-associated biomaterials. FEMS Microbiol Lett 173:279–284.
9. Costerton JW, Montanaro L, Arciola CR. 2005. Biofilm in implant infections: its production and regulation. Int J Artif Organs 28:1062–1068.
10. Mah TF, O'Toole GA. 2001. Mechanisms of biofilm resistance to antimicrobial agents. Trends Microbiol 9:34–39.
11. Kirby AE, Garner K, Levin BR. 2012. The relative contributions of physical structure and cell density to the antibiotic susceptibility of bacteria in biofilms. Antimicrob Agents Chemother 56:2967–2975.
12. Tiemann AH, Krenn V, Krukemeyer MG, et al. 2011. Infectious bone diseases. Pathologe 32:200–209.
13. Köckritz-Blickwede M von, Rohde M, Oehmcke S, et al. 2008. Immunological mechanisms underlying the genetic predisposition to severe *Staphylococcus aureus* infection in the mouse model. Am J Pathol 173:1657–1668.
14. Holstein JH, Garcia P, Histing T, et al. 2009. Advances in the establishment of defined mouse models for the study of fracture healing and bone regeneration. J Orthop Trauma 23:31–38.
15. Bjerkan G, WitsÄ E, Bergh K. 2009. Sonication is superior to scraping for retrieval of bacteria in biofilm on titanium and steel surfaces in vitro. Acta Orthop 80:245–250.
16. Hein I, Lehner A, Rieck P, et al. 2001. Comparison of different approaches to quantify *Staphylococcus aureus* cells by real-time quantitative pcr and application of this technique for examination of cheese. Appl Environ Microbiol 67:3122–3126.
17. Li D, Gromov K, Soballe K, et al. 2008. Quantitative mouse model of implant-associated osteomyelitis and the kinetics of microbial growth, osteolysis, and humoral immunity. J Orthop Res 26:96–105.
18. Pribaz JR, Bernthal NM, Billi F, et al. 2012. Mouse model of chronic post-arthroplasty infection: noninvasive in vivo bioluminescence imaging to monitor bacterial burden for long-term study. J Orthop Res 30:335–340.
19. Sottnik JL, U'Ren LW, Thamm DH, et al. 2010. Chronic bacterial osteomyelitis suppression of tumor growth requires innate immune responses. Cancer Immunol Immunother 59: 367–378.
20. Chen X, Tsukayama DT, Kidder LS, et al. 2005. Characterization of a chronic infection in an internally-stabilized segmental defect in the rat femur. J Orthop Res 23:816–823.
21. Schell H, Epari DR, Kassi JP, et al. 2005. The course of bone healing is influenced by the initial shear fixation stability. J Orthop Res 23:1022–1028. DOI: 10.1016/j.orthres.2005.03.005
22. Claes L, Eckert-Hubner K, Augat P. 2002. The effect of mechanical stability on local vascularization and tissue differentiation in callus healing. J Orthop Res 20:1099–1105.
23. Jabbouri S, Sadovskaya I. 2010. Characteristics of the biofilm matrix and its role as a possible target for the detection and eradication of *Staphylococcus epidermidis* associated with medical implant infections. FEMS Immunol Med Microbiol 59:280–291.

24. Evans CAW, Jellis J, Hughes SPF, et al. 1998. Tumor necrosis factor-α, interleukin-6, and interleukin-8 secretion and the acute-phase response in patients with bacterial and tuberculous osteomyelitis. J Infect Dis 177:1582–1587.
25. Klosterhalfen B, Peters KM, Tons C, et al. 1996. Local and systemic inflammatory mediator release in patients with acute and chronic posttraumatic osteomyelitis. J Trauma Acute Care Surg 40:372–378.
26. Bost KL, Ramp WK, Nicholson NC, et al. 1999. *Staphylococcus aureus* infection of mouse or human osteoblasts induces high levels of interleukin-6 and interleukin-12 production. J Infect Dis 180:1912–1920.
27. Ishimi Y, Miyaura C, Jin CH, et al. 1990. IL-6 is produced by osteoblasts and induces bone resorption. J Immunol 145: 3297–3303.

JOR – Journal of Orthopaedic Research

Impact Factor: 2.972

5-Year Impact Factor: 3.257

80 % eigener Anteil

1. Autor und Corresponding Author

Tieroperationen, Tierbetreuung, Röntgen, Labortätigkeit

PLOS ONE

RESEARCH ARTICLE

Lysostaphin-Coated Titan-Implants Preventing Localized Osteitis by *Staphylococcus aureus* in a Mouse Model

Ceylan D. Windolf[1]*, Tim Lögters[1], Martin Scholz[1,2], Joachim Windolf[1], Sascha Flohé[1]

1. Department of Trauma- and Hand Surgery, Heinrich-Heine University Duesseldorf, Moorenstr. 5, 40225, Duesseldorf, Germany, **2.** LEUKOCARE AG, Am Klopferspitz 19, 82152, Martinsried/Munich, Germany

*ceylan.windolf@uni-duesseldorf.de

OPEN ACCESS

Citation: Windolf CD, Lögters T, Scholz M, Windolf J, Flohé S (2014) Lysostaphin-Coated Titan-Implants Preventing Localized Osteitis by *Staphylococcus aureus* in a Mouse Model. PLoS ONE 9(12): e115940. doi:10.1371/journal.pone.0115940

Editor: Raymond Schuch, Rockefeller University, United States of America

Received: October 7, 2014

Accepted: December 2, 2014

Published: December 23, 2014

Data Availability: The authors confirm that all data underlying the findings are fully available without restriction. All relevant data are within the paper.

Funding: The work was financially supported by the "Zentrales Innnovationsprogramm Mittelstand" of the German ministry of economics and Technology; www.zim-bmwi.de; (KF2790101MK0); SF and the AO-Research foundation; https://www.aofoundation.org; (AO Start-Up grant S-11-34F); SF. They were not involved in study design; in the collection, analysis and interpretation of data; in the writing of the report; and in the decision to submit the article for publication.

Competing Interests: MS is associated with Department of Trauma- and Hand Surgery, Heinrich-Heine University Duesseldorf as well as employed by LEUKOCARE AG. The other authors confirm that there are no known conflicts of interest associated with this publication and there has been no significant financial support for this work that could have influenced its outcome. This does not alter the authors' adherence to PLOS ONE policies on sharing data and materials.

Abstract

The increasing incidence of implant-associated infections induced by *Staphylococcus aureus* (SA) in combination with growing resistance to conventional antibiotics requires novel therapeutic strategies. In the current study we present the first application of the biofilm-penetrating antimicrobial peptide lysostaphin in the context of bone infections. In a standardized implant-associated bone infection model in mice beta-irradiated lysostaphin-coated titanium plates were compared with uncoated plates. Coating of the implant was established with a poly(D,L)-lactide matrix (PDLLA) comprising lysostaphin formulated in a stabilizing and protecting solution (SPS). All mice were osteotomized and infected with a defined count of SA. Fractures were fixed with lysostaphin-coated locking plates. Plates uncoated or PDLLA-coated served as controls. All mice underwent debridement and lavage on Days 7, 14, 28 to determine the bacterial load and local immune reaction. Fracture healing was quantified by conventional radiography. On Day 7 bacterial growth in the lavages of mice with lysostaphin-coated plates showed a significantly lower count to the control groups. Moreover, in the lysostaphin-coated plate groups complete fracture healing were observed on Day 28. The fracture consolidation was accompanied by a diminished local immune reaction. However, control groups developed an osteitis with lysis or destruction of the bone and an evident local immune response. The presented approach of terminally sterilized lysostaphin-coated implants appears to be a promising therapeutic approach for low grade infection or as prophylactic strategy in high risk fracture care e.g. after severe open fractures.

Introduction

Implant-associated infections by SA are still a major challenge in trauma and orthopedic surgery even though modern operating standards and perioperative antibiotic applications minimize contamination during surgery [1]. In trauma and orthopedic surgery the presence of foreign surfaces of prosthesis or metal implants complicate the problem especially of chronified bone infections. The development of an osteomyelitis depends on both systemic host factors such as underlying diseases as diabetes, local vascularity and the degree of primary or secondary surgical tissue damage. So in general microorganisms cause an osteitis/osteomyelitis in the adult patient not alone but rather the interaction of invading microbials with an orthopedic device and the local immune response finally result in a persisting localized infection [2]. The biofilm formation of bacteria is the fundamental basis of such a chronically infected orthopedic implant [3]. Bacteria invade the host through an accidental wound or a surgical incision and attach on surfaces of implants by hydrophobic interactions [4]. There they accumulate to a multilayer cell cluster of sessile bacteria [4] and form a hydrated matrix of extracellular components including several proteins defined as biofilm [5–9]. This biofilm protects bacteria from the host's defenses and also dramatically increase their antibiotic resistance [1, 10–12]. Nevertheless, secreted protein-components of the biofilm matrix attract leukocytes and cause a local immune response. In the first line of defense, polymorphonuclear neutrophils (PMN) remain activated and secrete inflammatory factors which destroy bone and surrounding tissue [2, 13, 14] without clearing the infection. The term "frustrated phagocytosis" [15] coins the phenomenon quite well. Therefore biofilm infections are difficult to treat especially due to their inherent antibiotic resistance. Frequently, clearance of biofilm-associated infections necessitates complete implant removal. Hence, after primary attachment biofilm formation ought to be avoided [4]. In times of increasing antibiotic resistance and in the light of the failure of most antibiotic therapies alternative antimicrobial strategies becomes more and more important. One of these alternative antimicrobial substances is the antibacterial enzyme lysostaphin. Lysostaphin is a zinc ionic class III bacteriocin [16] with a molecular weight of 27 kDa [17], and contains 2 active enzymes: catalytic endopeptidase and cell wall binding domain (SH3b) [18, 19]. Lysostaphin may be able to target sessile bacteria in a biofilm and also directly destroys the extracellular biofilm matrix [20]. Pentaglycine cross bridges of cell wall components including polyglycines can be hydrolyzed by the glycylglycin endopeptidase function of lysostaphin [21]. Even methicillin-resistant SA can be rapidly eliminated avoiding undesirable systemic immune reactions [22]. The antibacterial potency of lysostaphin is well documented in animals and humans [23, 24]. Lysostaphin was applied intravenously in a rabbit model of aortic valve endocarditis [25]. The therapeutic efficacy was also demonstrated on implanted jugular vein catheters in mice [26] and in a SA induced keratitis and endophthalmitis in rabbits [27, 28]. Most SA strains are susceptible to lysostaphin due to less serine than glycine cell wall contents [21]. Although *Staphylococcus epidermidis* (SE) is known to be less

sensitive to lysostaphin, biofilm produced by these bacterial strains can also be destroyed by lysostaphin when applied in higher doses [29]. In contrast lysostaphin had no visible effects on biofilms produced by *Pseudomonas aeruginosa in vitro* [29]. The systemic therapeutic application of lysostaphin may be limited by adverse side effects of the host's immune system reacting on a recombinant protein. In the context of the prevention or treatment of a localized infection at the implant/tissue interface an antimicrobial coating of implants with substances like lysostaphin seems to be a promising option. However, the prerequisite of stable and terminally sterilized bio-functionalized lysostaphin coated metal implant has so far not been addressed systematically. Therefore, the aim of this study was to evaluate an orthopedic device coated with polylactid acid in combination with stabilized lysostaphin in order to inhibit the growth of SA and to avoid implant-associated bone infections in a standardized animal model.

Materials and Methods

Titanium plate coating

Titanium discs grade 1 (ARA-T Advance GmbH, Dinslaken, Germany) with a size of 20×2 mm were coated with 1 mg/ml lysostaphin (ProSpec, East Brunswick, NJ, USA) per disc in a poly(D,L)-lactide (PDLLA) matrix. Lysostaphin was rebuffered in a protecting amino acid–based composition derived from the stabilizing and protecting solution platform (SPS, LEUKOCARE AG, Munich, Germany). PDLLA was dissolved in ethyl acetate (133 mg/ml) and mixed with lysostaphin to obtain a final concentration of 1 mg/ml. The loading of PDLLA on titanium plates was 17,5 µg Lysostaphin/mm^2 and 2,33 mg PDLLA/mm^2. The surface of the implants was 8 mm^2 and therefore the total loading per implant was 40 µg lysostaphin and 18,64 mg PDLLA. The thickness of the lysostaphin-PDLLA coated plates using a standard coating protocol for PDLLA coatings was approximately 10 µm [30, 31, 32]. Titanium plates were cleaned with 30% (v/v) Piranha solution, a mixture of 30% hydrogen peroxide and concentrated sulfuric acid (98% H_2SO_4) and washed with PBS three times. Subsequently, titanium plates were dipped in the PDLLA-lysostaphin mixture (LEUKOCARE AG) and air-dried. This dip-drying step was repeated two times to obtain a multi-layer comprising PDLLA and lysostaphin. After the final drying step the coated titanium plates were sterilized with 40 kGy beta irradiation (BGS, Saale an der Donau, Germany). Terminally sterilized lysostaphin-coated titanium plates were used in microbiological screening assays and animal experiments within two weeks.

Bacterial growth inhibition on titanium plates in vitro

The biofilm forming SA strain ATCC 29213 was cultivated in BactoTryptic Soy Broth overnight and afterwards diluted 1:100. The coated titanium discs and uncoated control discs were incubated in the bacterial culture for 48 h at 37℃ and

constantly moved at 100 rpm. Bacteria were enumerated based on colony-forming units (CFU). In order to confirm the transferability into the *in vivo* osteitis mouse model titanium 4-hole MouseFix plates (RISystem, Davos, Switzerland) were coated as described before and one group of plates was additionally irradiated with 40 kGy-β for sterilization. Antibacterial activity of the implant and bacterial growth was analyzed as described above for titanium discs.

Animals

For the experiments ten to twelve-week-old female wild-type Balb/c mice with an average weight of 21g were used (animal core facility of the Heinrich-Heine-University Duesseldorf; Germany). All animal procedures were carried out in accordance to local and national ethical guidelines and were approved by the regional ethical committee, Regional Office for Nature, Environment and Consumer Protection Nordrhein-Westfalen, Germany, with the ethical approval ID 87-51.04.2010.A112.

Low Grade Acute Osteitis Model

A previously established implant-associated osteitis model in mice [33] was used for *in vivo* testing of coated titanium implants. Briefly, mice were anesthetized by i.p. injection of xylazine (25 mg/kg body weight) and ketamine (75 mg/kg body weight). After skin incision under sterile conditions, the fascia was opened, and the MouseFix plate was fixed to the femur. Four different treatment groups (n=10 mice/group) were investigated: One group received titanium plates coated with 1 mg/ml lysostaphin in PDLLA per plate. One group received titanium plates coated with 1 mg/ml lysostaphin in PDLLA per plate with additional irradiation with 40 kGy-β for terminal sterilization. One control group received uncoated plates and another control group received titanium plates coated only with PDLLA. After plate fixation an osteotomy using a Gigly saw (diameter 0.22 mm, RISystem) was performed in midshaft of the femur to create a bone defect. Subsequently, 1 µl SA strain ATCC 29213 with an average CFU of 1.94E+03/µl was inoculated into the fracture gap. All mice were anesthetized again 7 and 14 days after primary operation and standardized lavage (250 µl PBS twice) with debridement of infected tissue was performed. The lavage fluid was recovered and PBS added to a total volume of 1 ml. Local debridement was performed with a surgical spoon without involving the periosteum. All surgical interventions were made by the same surgeon. At Day 28 animals were sacrificed, blood was gained by cardiac puncture and a final lavage was collected from the surgical field.

Counts of Colony-Forming Units (CFU)

The number of colony-forming units (CFU) was elevated in the lavage on Day 7, 14, and 28. Bacteria from the thigh were gained by lavage under aseptic conditions as described before. 200 µl of lavage were serially diluted in PBS and four

replicates of 10 µl of each dilution plated on Columbia agar plates with 5% sheep blood. The plates were incubated for 24 h at 37℃, and afterwards colonies were counted. Results are expressed in CFU/ml lavage fluid.

Radiographic Analysis

On Days 0, 7, 14, and 28 after plate fixation anteroposterior radiographic images (MX20 Faxitron, Tucson, Arizona, USA) of the femora were taken. In order to rate the bone healing on radiographs we developed a score to the fracture gap size. The fracture gap size was measured at the plate opposing corticalis. The MouseFix plate has a length of 8 mm. This internal standard allows an exact calculation of the diameter of the fracture gap (Adobe Photoshop CS6). Decreasing diameters of fracture gaps representing fracture healing were rated with 1 point; a constant fracture gap meaning no healing was rated with 2 points, increasing facture gaps were rated with 3 points, obvious osteolysis with 4 and destruction of the bone were rated with 5 points.

Analysis of Local Immune Response

The local immune response was characterized by measuring total leucocytes and PMNs in the lavage using flow cytometry (FACSCalibur BD Biosciences, Heidelberg, Germany). For neutrophilic granulocyte characterization, forward and side scatter characteristics and the myeloid cell marker APC rat anti-mouse CD11b (BD Pharmingen, Frankfurt, Germany, monoclonal, catalog number: 553991, clone: A95-1) were used.

Quantification of IL-6 by ELISA

IL-6 levels in the lavage were analyzed (VICTOR Multilabel Counter, PerkinElmer LAS, Rodgau, Germany) using a commercially available IL-6 ELISA kit according to the manufacturer's instructions (R&D Systems, Abingdon, UK, catalog number: DY406). The lower detection limit for IL-6 was 7.5 pg/ml.

Statistical Methods

All data are expressed as median and whiskers min to max or mean and SEM. Omnibus normality test by D'Agostino and Pearsons. Data were tested for statistical significance with two-tailed Student's t-test, Mann-Whitney-test or Wilcoxon-test using GraphPad Prism5 (GraphPad Software, San Diego, CA): p values ≤ 0.05 were considered as significant.

Results

Lysostaphin Retain Activity after Coating on Titan Discs

First, the successful coating of lysostaphin on titanium discs was demonstrated. Bacterial culture with uncoated titanium discs revealed a median of 5.6E+07 CFU (n=50) after 48 h incubation. In contrast, only 6 of 42 bacterial cultures with lysostaphin-coated discs showed any bacterial growth while the remaining 36 cultures were sterile after 48 h incubation (Fig. 1). Correspondingly, almost all lysostaphin-coated mouse fix plates were sterile after 48 h incubation. Only, two of 10 cultured MouseFix plates revealed bacteria growth after 48 h independent of irradiation (Fig. 2).

Bacterial Growth and Bone Healing

CFU counts in the lavage around the fracture site were measured on Days 7, 14, and 28 after primary surgery. Both the lavages of mice with uncoated plates and with the PDLLA coated control plates revealed a high and persistent bacterial load over the whole observation period of four weeks. There was no difference between mice groups with uncoated and PDLLA coated plates. However, in all mice groups with lysostaphin-coated plates bacterial growth in lavage revealed a significantly lower rate at any time point. Most lavages of the lysostaphin-coated plates were sterile (Fig. 3). Accordingly, radiographs of femora from mice with lysostaphin-coated plates showed clear signs of fracture healing by Day 14 and complete fracture consolidation by Day 28. In contrast, in all mice with uncoated or only PDLLA coated control plates fracture healing could not be observed at any time point (Fig. 4). The fracture gap was evaluated using a semi quantitative score as described above. Mice with lysostaphin-coated plates displayed a significantly higher bony healing compared to control animals. Indeed, all control groups developed clear signs of an osteitis with osteolysis or destruction of the femora (Fig. 5).

Immune Response

The number of leukocytes in the lavage of mice with lysostaphin-coated plates on Days 7, 14, and 28 was significantly lower than in the control groups (Fig. 6). In lysostaphin-coated implants leukocytes further decreased over time while in the uncoated control groups persistent high number of leukocytes were detectable in the lavage. In the control groups leukocytes predominantly consisted of PMNs (more than 80% at any time point). The percentage of neutrophils in the lavage was significantly lower in the lysostaphin groups (Fig. 7) at all times.

High numbers of IL-6 were found in the lavages on day 7 in both infected control groups without lysostaphin-coated implants which continuously decreased over time. However, also on the 28th day there were still considerable numbers of IL-6 present in the lavage. In contrast IL-6 was barely detectable at any time points in all lavages of lysostaphin-coated implants (Fig. 8).

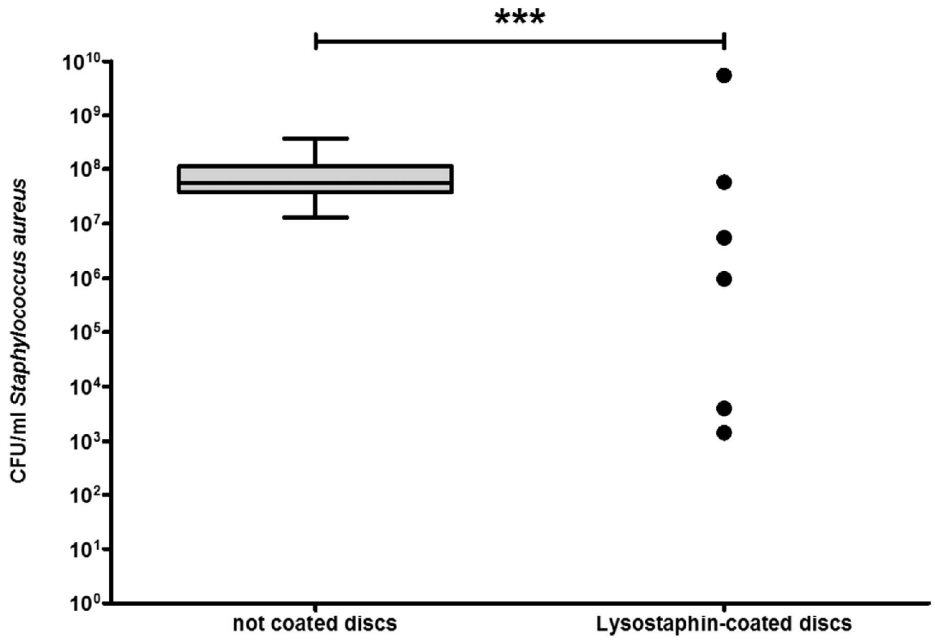

Fig. 1. Lysostaphin-coating of titanium discs prevents bacterial growth. Titanium discs were incubated with in SA strain ATCC 29213 for 48 h. 36 of 42 cultures with lysostaphin-coated discs were sterile and thus only the six positive cultures are shown. The median CFU of cultures with uncoated discs (n=50) was 5.62E+07 ($p<0.0001$). CFU are presented as box plots with median and whiskers min to max. Statistical analysis was performed using two-tailed Mann-Whitney-test.

doi:10.1371/journal.pone.0115940.g001

Discussion

Osteomyelitis of implant-associated infection remains one of the major challenges in musculoskeletal surgery. Especially in severe open fractures bacterial contamination continues to be a major cause for non-union, local infection or even sepsis. Surgical debridement and antibiotic therapy are the most important treatments to control bacterial contamination. However, the efficacy of local or systemic therapy with most antibiotics in terms of eradication of surface-attached bacterial colonies with biofilm formation is very limited due to the slow growth and metabolic rate of biofilm-associated bacterial colonies [34]. Since foreign surfaces in form of metal implants are inevitably combined with fracture stabilization, biofilm-associated bacteria on the surface of orthopedic fixation devices contribute to persistent or recurrent local bone infection and delayed or missing fracture union [35]. Due to the increasing incidence of infections in orthopedic implants and growing occurrence of resistant bacteria the search for new methods to avoid implant-associated infections becomes of major importance. Novel approaches include anti-adhesive polymers, bioactive biomaterials such as chitosan derivatives or polycationic polymers and bioactive coatings with e.g. NO releasing silica nanoparticles, excellently summarized by Campoccia [36, 37]. So far most of these innovative approaches are evaluated only *in vitro* merely focusing on the bacterial growth on the foreign surface.

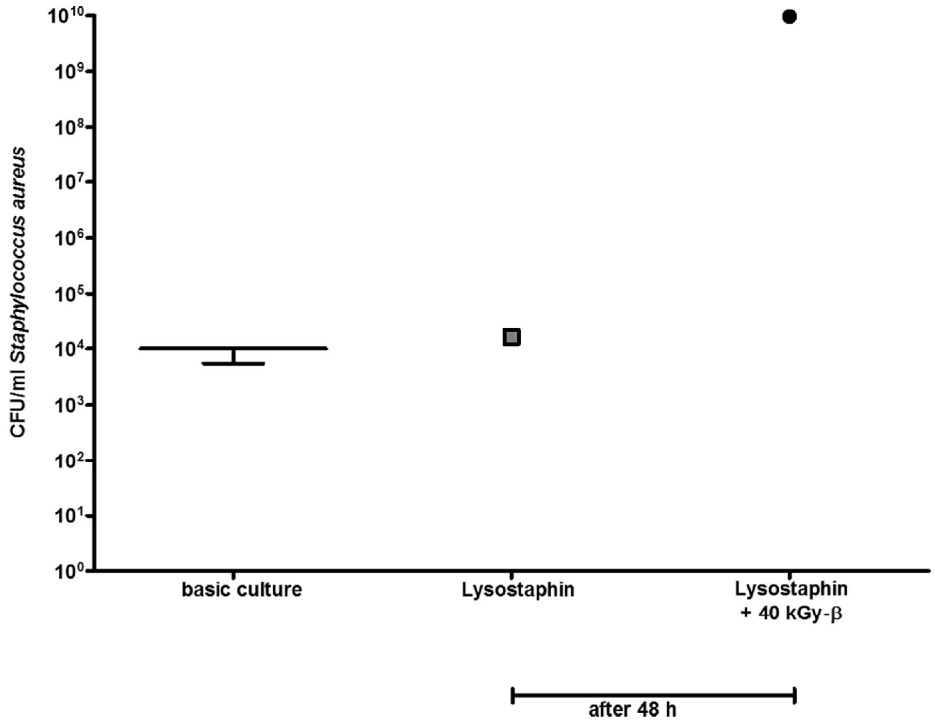

Fig. 2. The coating method of the titan discs was transferable to the MouseFix plate. In 4 of 5 cultures of each group (MouseFix plates coated with lysostaphin and MouseFix plates coated with lysostaphin and sterilized with 40 kGy beta irradiation) no bacterial growth was measured after 48 h cultivation in a basic culture of SA with 1.00E+04 CFU/ml and thus only one positive culture of each group is shown.

doi:10.1371/journal.pone.0115940.g002

Based on epidemiological studies SA strains are the most frequent cause of bone infection especially in context with metal devices [6, 38, 39]. SA is known to be a potent biofilm former which further contributes to the complexity of such an infection [2]. Methicillin-resistant SA additionally limits the systemic therapeutic possibilities and therefore is a common cause for missing osseous union or even extremity amputation. This scenario calls for biofilm-penetrating substances with bactericidal activity especially against SA. The bactericidal peptide lysostaphin fulfills both prerequisites. Therefore we analyzed lysostaphin-coated metal implant in SA infection both *in vitro* and *in vivo* in a model of acute implant-associated bone infection. Surface binding of bioactive lysostaphin was accomplished with a PDLLA-carrier. PDLLA as carrier for antibiotics like gentamycin or norvancomycin [40–42] or pharmaceuticals like zoledronic acid [43] or growth factors like TGF-β [44] *in vitro* is well established. PDLLA is biocompatible, durable on implants, and does not induce any undesirable immune reactions [45]. However, PDLLA-dependent coating of lysostaphin has not been described before.

The two stereoisomers of lactic acid, L-lactic acid and D-lactic acid can produce four distinct materials: Poly(*D*-lactic acid) (PDLA), a crystalline material with a regular chain structure; poly(*L*-lactic acid) (PLLA), which is hemicrystalline, and

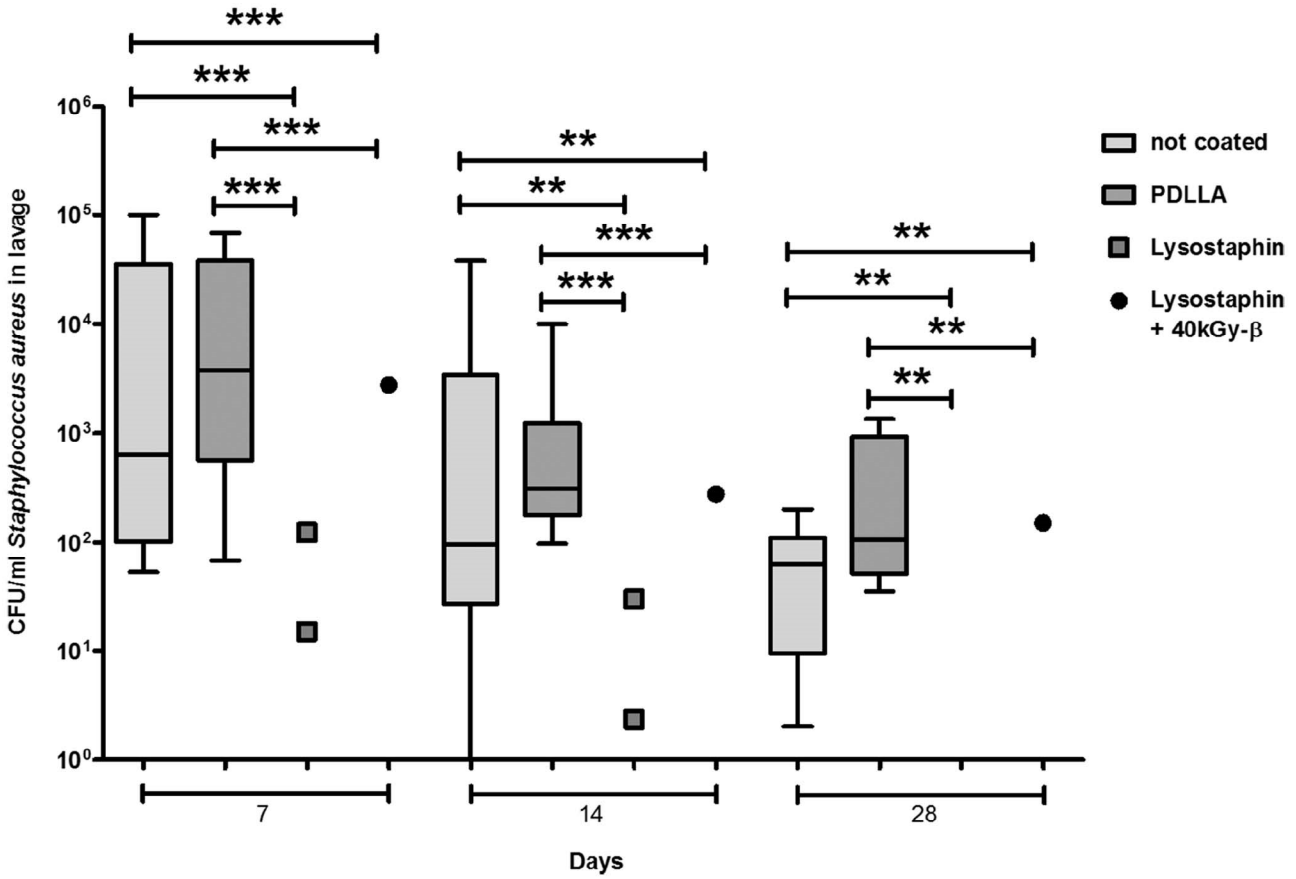

Fig. 3. Local detection of SA around the fracture side of mice. Both groups with lysostaphin coated plates showed a significant lower bacterial count to the control groups (mice with uncoated plates, and mice with only PDLLA coated plates) at all times. In only 2 of nine respectively 1 of nine lavages in mice with lysostaphin coated plates bacterial growth was detectable with decreasing count from Day 7 to 28; all other lavages were sterile at any time. $^{**}p<0.01$, $^{***}p<0.001$. CFU are presented as box plots with median and whiskers min to max. Statistical analysis was performed using two-tailed Mann-Whitney-test and Wilcoxon-test.

doi:10.1371/journal.pone.0115940.g003

likewise with a regular chain structure; poly(*D,L*-lactic acid) (PDLLA) which is highly hydrophobic and amorphous; and *meso*-PLA, obtained by the polymerization of *meso*-lactide. PDLA, PLLA and PDLLA are soluble in common solvents including ethyl acetate, benzene, chloroform, dioxane, etc. and degrade by simple hydrolysis of the ester bond even in the absence of a hydrolase [46, 47]. In this work the coating is based on an amorphous polymer of low molecular weight poly(D,L-lactic acid), Resomer R203H with molecular weights M_w between 18000–24000 Da. Surprisingly, SPS-formulated lysostaphin remained stable and bioactive after PDLLA coating even after terminal sterilization of the coated implants by 40 kGy beta-radiation. From the regulatory point of view, terminal sterilization is required for the approval of medical devices whenever it is achievable. Moreover, increased stability of biomolecule-coated implants may prevent storage-related loss of function. Embedding the SPS-stabilized antibacterial enzyme lysostaphin in the dried amorphous matrix of poly(D,L-lactide)

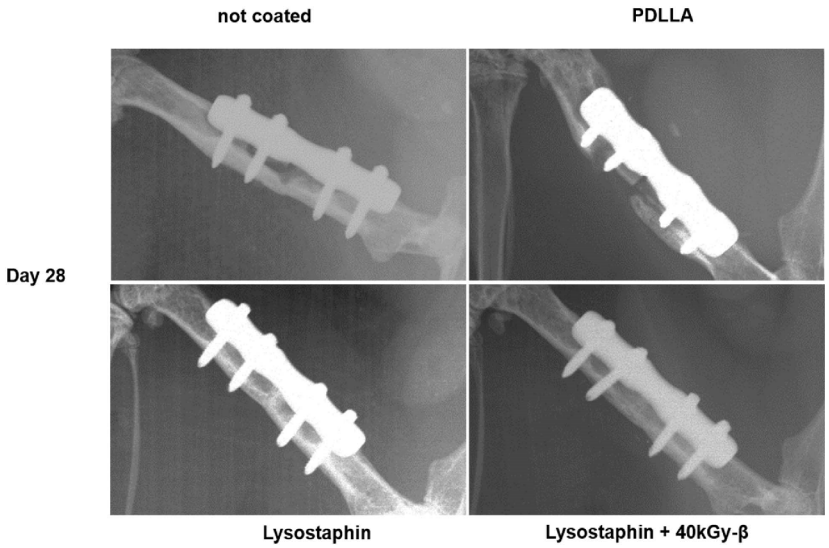

Fig. 4. Representative x-rays of the fracture zone on Day 28. A consolidation of the fracture gap on Day 28 in both mice groups with lysostaphin-coated plates in contrast to the control groups (mice with uncoated plates, and mice with only PDLLA coated plates) after osteotomy, plate fixation and inoculation of SA with an average CFU of 1.94E+03/μl is demonstrated.

doi:10.1371/journal.pone.0115940.g004

might be an interesting approach to clinically address the formation of SA-related

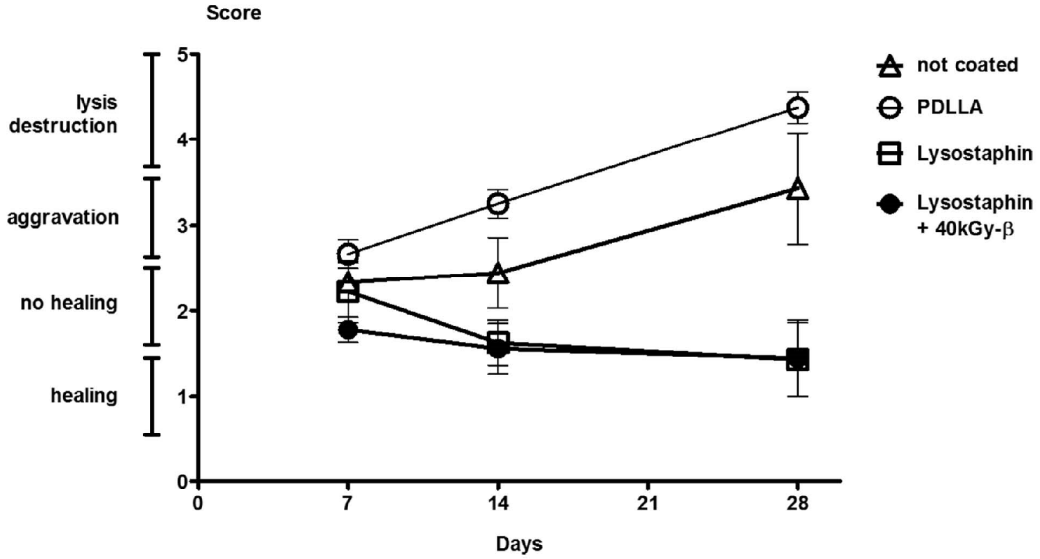

Fig. 5. Score of fracture healing. Standardized radiographic quantification of fracture healing from mice groups with lysostaphin-coated plates (n=51) vs. control groups (n=50) on Days 7, 14, and 28 after osteotomy, fracture fixation and inoculation of SA. Significant differences on Day 7: not coated vs. lysostaphin +40 kGy-β (p=0.0340), PDLLA vs. lysostaphin (p=0.0211), PDLLA vs. lysostaphin +40 kGy-β (p=0.0017). On Day 14: PDLLA vs. lysostaphin (p=0.0009), PDLLA vs. lysostaphin +40 kGy-β (p=0.0014). On Day 28: not coated vs. lysostaphin (p=0.0186), not coated vs. lysostaphin +40 kGy-β (p=0.0186), PDLLA vs. lysostaphin (p=0.0014), PDLLA vs. lysostaphin +40 kGy-β (p=0.0022). Radiographic quantifications are presented as mean and SEM. Statistical analysis was performed using one-tailed Mann-Whitney-test.

doi:10.1371/journal.pone.0115940.g005

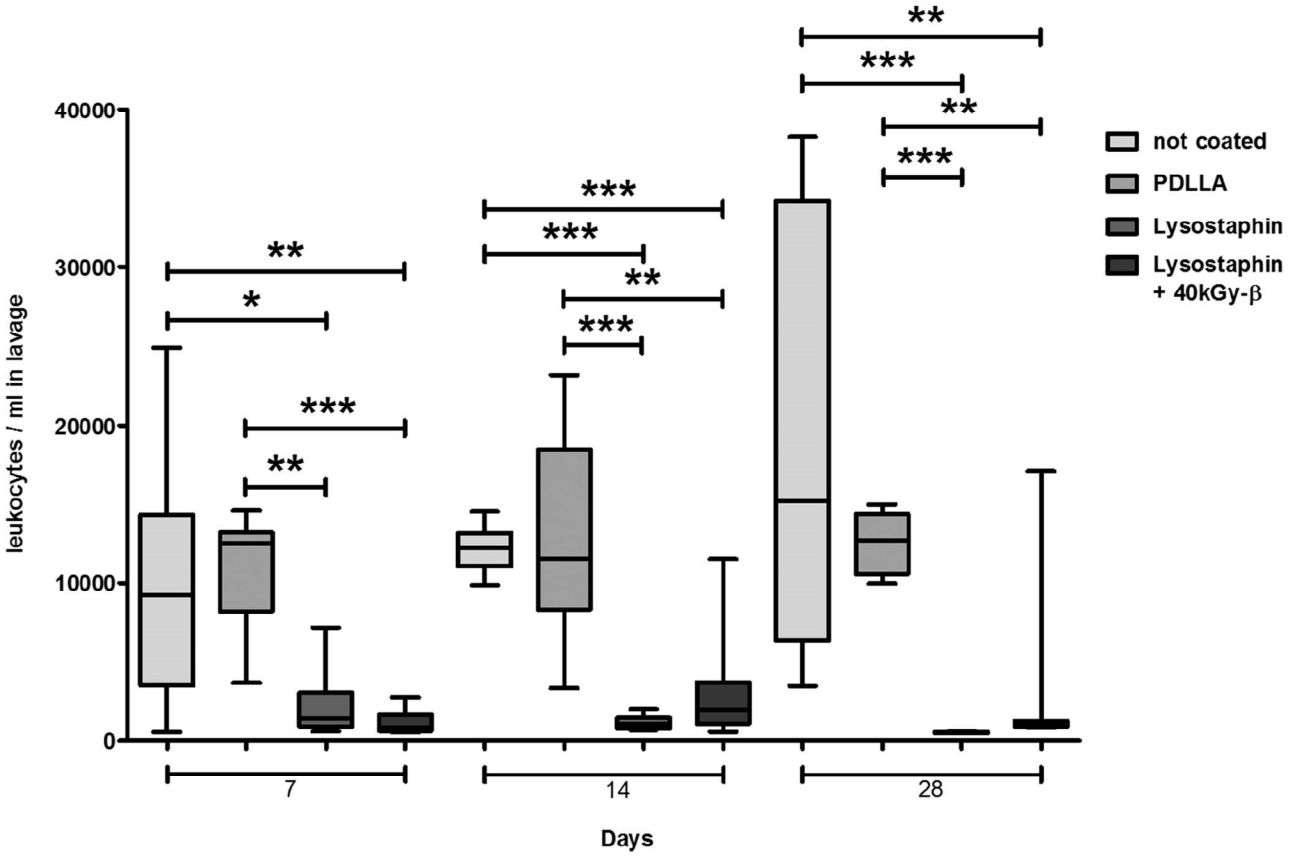

Fig. 6. Detection of leukocytes in lavage fluid. Significantly lower counts of leukocytes in lavages of both mice groups with lysostaphin-coated plates (n=52) versus control groups (mice with uncoated plates, and mice with only PDLLA coated plates; n=49). *$p<0.05$, **$p<0.01$, ***$p<0.001$. Statistical analysis was performed using two-tailed Student's t-test and Mann-Whitney-test.

doi:10.1371/journal.pone.0115940.g006

biofilms on implants in the future.

In this work we demonstrated for the first time the successful coating of lysostaphin on titan implants and its effectiveness in an *in vivo* mouse model. Bacterial growth of the contaminated fracture gap was almost completely avoided. Consecutively, osseous consolidation was achieved with lysostaphin-coated implants in spite of the initial bacterial contamination. In addition, infection-associated local inflammation was also prevented by the application of a lysostaphin-coated implant. At least in this mouse model of acute bone infection lysostaphin-coated implants seem to be a very promising therapeutic approach.

The potency of lysostaphin has been described in several local applications, i.e. as cream to reduce nasal colonization in rat [48]. Intravenous application of lysostaphin can reduce systemic- and organ infections in mice [49]. Lysostaphin disrupts biofilm *in vitro* and additionally acts bactericidal to SA strains and with a smaller efficacy also to SE [20]. Nevertheless, lysostaphin will not be the ultimate miracle cure for all musculoskeletal infections. Until now, only few lysostaphin-resistant SA strains have been reported but mutations to a higher amount of

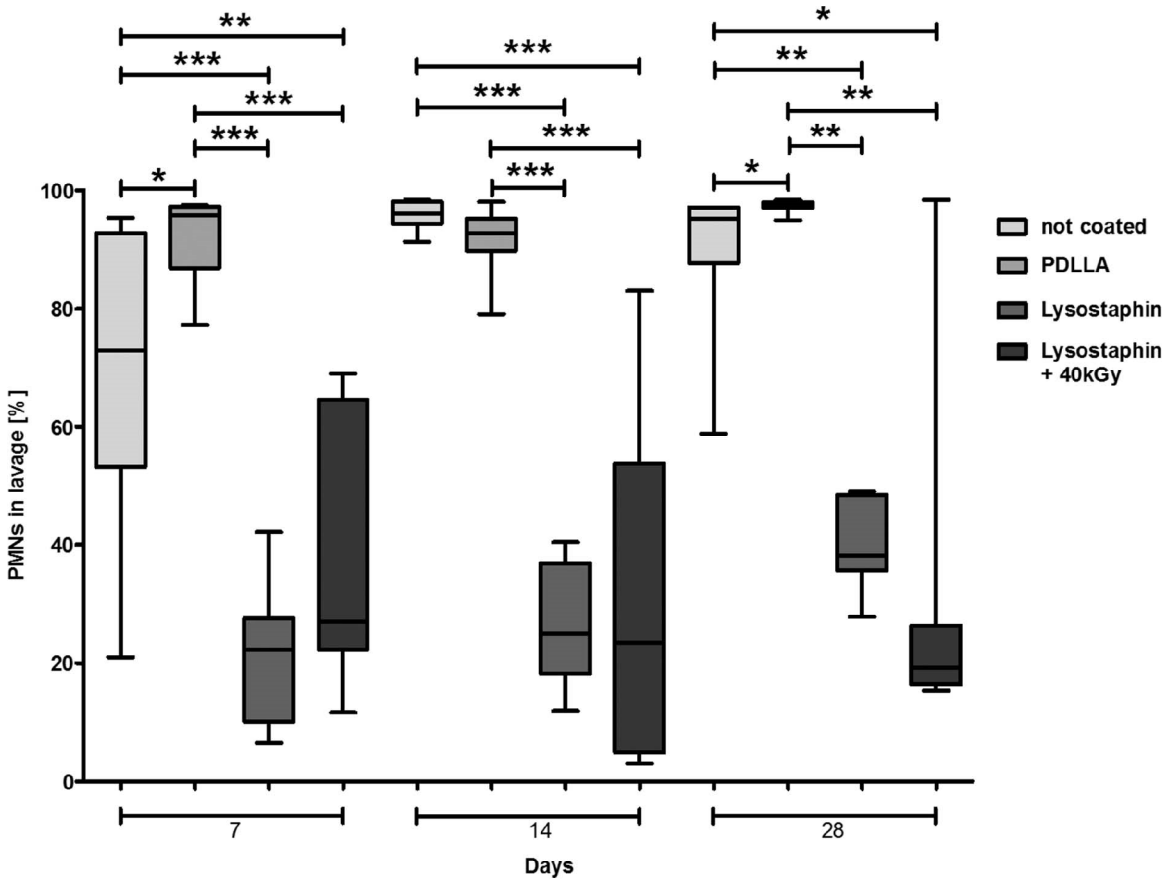

Fig. 7. Percentage distributions of neutrophils in lavage fluid. In mice groups with lysostaphin-coated plates (n=52) are less neutrophils than in the control groups (n=49). *p<0.05, **p<0.01, ***p<0.001. Statistical analysis was performed using two-tailed Student's t-test and Mann-Whitney-test.

doi:10.1371/journal.pone.0115940.g007

serine in the peptidoglycan of SA cell wall will result in diminishing anti-staphylococcal effect of this substance [21]. In addition, antibacterial efficacy of lysostaphin is limited to SA and in higher concentration to SE. So far only metal implants coated with agents like vancomycin or gentamycin are available. However, both of these antibiotics do not penetrate biofilm [50, 51]. In the context of the biofilm-associated infection coatings with vancomycin or gentamycin do not seem to be the perfect choice of antibiotic substance. But a combination of the glycopeptide antibiotics vancomycin or gentamycin with lysostaphin would be a potential weapon against SA even after biofilm formation [25].

Of course the lysostaphin-coated implants as described in this experimental series have some limitations. Firstly, we were not able to achieve a sterile culture in all samples *in vitro* as an evidence for some inconsistency in the drug-eluting efficacy of the PDLLA-coating procedure. Secondly, long term stability of the PDLLA-lysostaphin-coating needs to be evaluated. Further, in the experimental set up lysostaphin-coated implants were present with the onset of the infection.

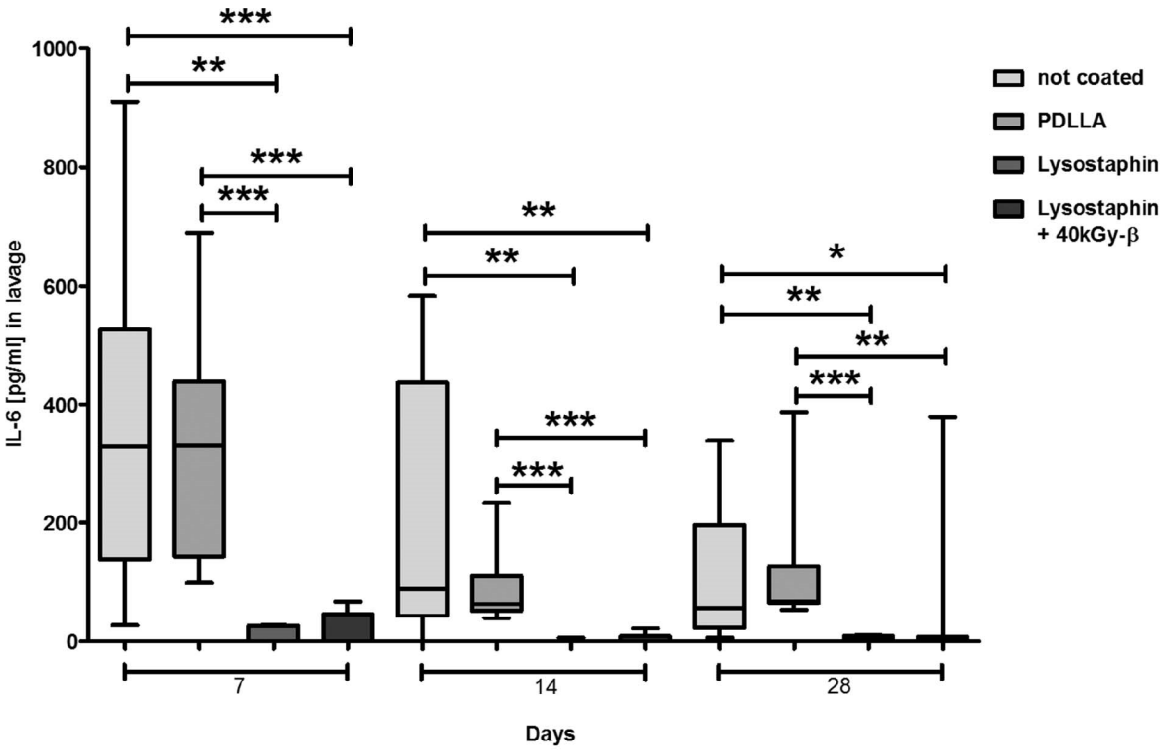

Fig. 8. Detection of IL-6 in lavage fluids. IL-6 in lavage of both mice groups with lysostaphin-coated plates ($n=52$) were only detectable to a minor degree in contrast to the control groups (mice with uncoated plates, and mice with only PDLLA coated plates; $n=49$). *$p<0.05$, **$p<0.01$, ***$p<0.001$. Statistical analysis was performed using two-tailed Student's t-test and Mann-Whitney-test.

doi:10.1371/journal.pone.0115940.g008

Therefore, the presented data actually do not allow any conclusions concerning the efficacy of lysostaphin in an established bone infection. Based on the presented *in vivo* data however, we can demonstrate that lysostaphin-coating completely prevents the development of an osteomyelitis in spite of a significant bacterial contamination and the presence of a metal surface, normally leading to persisting infections due to biofilm formation. From a clinical point of view such a strategy is quite realistic. Antimicrobial coating of orthopedic fixation devices would be desirable in open fracture treatment or in high risk osteosynthesis e.g. in elderly patients with an impaired immune response. In addition, after the infection has been clinically resolved such an antimicrobial coating of an implant would be of special use in septic bone surgery to ensure a minimized risk of reinfection after secondary internal fixation. In such situations an antimicrobial coating of the implant could be of interesting choice to avoid recurrence of infection. The same holds true for the emerging problem of septic revision arthroplasty.

Conclusion

Biofilm-associated bone infections prevent osseous consolidation and are a significant problem e.g. in the treatment of open fractures. Lysostaphin, as a potential therapeutic agent coated on implant surfaces with a common carrier like PDLLA avoids an osteitis in mice femur and results in a complete consolidation of a fracture gap in spite of inoculation with SA.

Therefore, lysostaphin-coated fixation devices are a promising therapeutic strategy for open fractures or septic revision surgery.

Acknowledgments

We thank K. Kemter (LEUCOCARE AG) for coating plates. C. R. MacKenzie, K. Pfeffer, J. Hegemann and M. Hoffmann for valuable advice.

Author Contributions

Conceived and designed the experiments: CDW TL MS JW SF. Performed the experiments: CDW. Analyzed the data: CDW TL MS JW SF. Contributed reagents/materials/analysis tools: CDW TL MS JW SF. Wrote the paper: CDW TL MS JW SF.

References

1. **Campoccia D, Montanaro L, Arciola CR** (2006) The significance of infection related to orthopedic devices and issues of antibiotic resistance. Biomaterials 27:2331–2339.
2. **Montanaro L, Testoni F, Poggi A, Visai L, Speziale P, et al.** (2011) Emerging pathogenetic mechanisms of the implant-related osteomyelitis by Staphylococcus aureus. Int J Artif Organs 34:781–788.
3. **Costerton JW, Stewart PS, Greenberg EP** (1999) Bacterial Biofilms: A Common Cause of Persistent Infections. Science 284:1318–1322.
4. **Arciola CR, Campoccia D, Speziale P, Montanaro L, Costerton JW** (2012) Biofilm formation in Staphylococcus implant infections. A review of molecular mechanisms and implications for biofilm-resistant materials. Biomaterials 33:5967–5982.
5. **Cucarella C, Solano C, Valle J, Amorena B, Lasa I, et al.** (2001) Bap, a Staphylococcus aureus surface protein involved in biofilm formation. J Bacteriol. 183:2888–2896.
6. **Götz F** (2002) Staphylococcus and biofilms. Mol Microbiol. 43:1367–1378.
7. **Yarwood JM, Schlievert PM** (2003) Quorum sensing in Staphylococcus infections. J Clin Invest. 112:1620–1625.
8. **Costerton JW, Montanaro L, Arciola CR** (2005) Biofilm in implant infections: its production and regulation. Int J Artif Organs 28:1062–1068.
9. **O'Gara JP** (2007) ica and beyond: biofilm mechanisms and regulation in Staphylococcus epidermidis and Staphylococcus aureus. FEMS Microbiol. Lett. 270(2):179–188.
10. **An YH, Friedman RJ** (1998) Concise review of mechanisms of bacterial adhesion to biomaterial surfaces. J Biomed Mater Res. 43:338–348.
11. **Hudson MC, Ramp WK, Frankenburg KP** (1999) Staphylococcus aureus adhesion to bone matrix and bone-associated biomaterials. FEMS Microbiol. Lett. 173:279–284.

12. **Kirby AE, Garner K, Levin BR** (2012) The Relative Contributions of Physical Structure and Cell Density to the Antibiotic Susceptibility of Bacteria in Biofilms. Antimicrob. Agents and Chemother. 56:2967–2975.

13. **Wagner C, Kondella K, Bernschneider T, Heppert V, Wentzensen A, et al.** (2003) Post-traumatic osteomyelitis: analysis of inflammatory cells recruited into the site of infection. Shock 20:503–510.

14. **Wagner C, Obst U, Hänsch GM** (2005) Implant-associated posttraumatic osteomyelitis: collateral damage by local host defense? Int J Artif Organs 28:1172–1180.

15. **Sadowska B, Więckowska-Szakiel M, Paszkiewicz M, Różalska B** (2013) The Immunomodulatory Activity of Staphylococcus aureus Products Derived from Biofilm and Planktonic Cultures. Arch. Immunol. Ther. Exp. (Warsz.) 61:413–420.

16. **Bastos MdCF de, Coutinho BG, Coelho MLV** (2010) Lysostaphin: A Staphylococcal Bacteriolysin with Potential Clinical Applications. Pharmaceuticals 3:1139–1161.

17. **Trayer HR, Buckley CE 3rd** (1970) Molecular properties of lysostaphin, a bacteriolytic agent specific for Staphylococcus aureus. J Biol Chem. 245:4842–4846.

18. **Gargis SR, Heath HE, LeBlanc PA, Dekker L, Simmonds RS, et al.** (2010) Inhibition of the Activity of Both Domains of Lysostaphin through Peptidoglycan Modification by the Lysostaphin Immunity Protein. Appl Environ Microbiol. 76:6944–6946

19. **Sabala I, Jagielska E, Bardelang PT, Czapinska H, Dahms SO, et al.** (2014) Crystal structure of the antimicrobial peptidase lysostaphin from Staphylococcus simulans. FEBS J 281:4112–4122

20. **Walencka E, Sadowska B, Rozalska S, Hryniewicz W, Rozalska B** (2005) Lysostaphin as a potential therapeutic agent for staphylococcal biofilm eradication. Pol J Microbiol. 54:191–200.

21. **Kumar JK** (2008) Lysostaphin: an antistaphylococcal agent. Appl Microbiol Biotechnol. 80:555–561.

22. **Dajcs JJ, Thibodeaux BA, Girgis DO, Shaffer MD, Delvisco SM, et al.** (2002) Immunity to lysostaphin and its therapeutic value for ocular MRSA infections in the rabbit. Invest Ophthalmol Vis Sci 43:3712–3716.

23. **Schindler CA, Schuhardt VT** (1964) Lysostaphin: A New Bacteriolytic Agent for the Staphylococcus. Proc Natl Acad Sci U S A. 51:414–421.

24. **Pulverer G** (1968) Untersuchungen mit Lysostaphin. II. Lysostaphin-Empfindlichkeit von 230 Staph. aureus-Stämmen tierischer Herkunkt. Z. med. Mikrobiol.u. Immunol. 154:49–53.

25. **Climo MW, Patron RL, Goldstein BP, Archer GL** (1998) Lysostaphin treatment of experimental methicillin-resistant Staphylococcus aureus aortic valve endocarditis. Antimicrob Agents Chemother. 42:1355–1360.

26. **Kokai-Kun JF, Chanturiya T, Mond JJ** (2009) Lysostaphin eradicates established Staphylococcus aureus biofilms in jugular vein catheterized mice. J Antimicrob. Chemother. 64:94–100.

27. **Dajcs JJ, Hume EB, Moreau JM, Caballero AR, Cannon BM, et al.** (2000) Lysostaphin treatment of methicillin-resistant Staphylococcus aureus keratitis in the rabbit. Invest Ophthalmol Vis Sci 41:1432–1437.

28. **Dajcs JJ, Thibodeaux BA, Hume EB, Zheng X, Sloop GD, et al.** (2001) Lysostaphin is effective in treating methicillin-resistant Staphylococcus aureus endophthalmitis in the rabbit. Curr Eye Res. 22:451–457.

29. **Wu JA, Kusuma C, Mond JJ, Kokai-Kun JF** (2003) Lysostaphin disrupts Staphylococcus aureus and Staphylococcus epidermidis biofilms on artificial surfaces. Antimicrob Agents Chemother. 47:3407–3414.

30. **Lakdawala M, Hassan PA, Devesh K, Malik GM** (2013) Poly(D,L-Lactide)-Gentamicin composite coated orthopaedic metallic implant. International Journal of Science and Nature 4:522–529

31. **Raschke MJ, Fuchs T, Stange R, Lucke M, Kandziora E, et al**, (2006) Active Coating of implants used in Orthopedic Surgery. In Leung K S, Taglang G, Schnettler R, (eds.), Practice of Intramedullary Locked Nails pp, 283–296

32. **Strobel C, Schmidmaier G, Wildemann B** (2011) Changing the release kinetics of gentamicin from poly(D,L-lactide) implant coatings using only one polymer. Int J Artif Organs 34:304–316

33. **Windolf CD, Meng W, Lögters TT, MacKenzie CR, Windolf J, et al.** (2013) Implant-associated localized osteitis in murine femur fracture by biofilm forming Staphylococcus aureus. A novel experimental model. J Orthop.Res. 31:2013–2020.

34. **Garcia LG, Lemaire S, Kahl BC, Becker K, Proctor RA, et al.** (2013) Antibiotic activity against small-colony variants of Staphylococcus aureus: review of in vitro, animal and clinical data. J Antimicrob. Chemother. 68:1455–1464.

35. **Meghji S, Crean SJ, Hill PA, Sheikh M, Nair SP, et al.** (1998) Surface-associated protein from Staphylococcus aureus stimulates osteoclastogenesis: possible role in S. aureus-induced bone pathology. Br J Rheumatol. 37:1095–1101.

36. **Campoccia D, Montanaro L, Arciola CR** (2013) A review of the biomaterials technologies for infection-resistant surfaces. Biomaterials 34:8533–8554.

37. **Goodman SB, Yao Z, Keeney M, Yang F** (2013) The future of biologic coatings for orthopaedic implants. Biomaterials 34:3174–3183.

38. **Stefansdottir A, Johansson D, Knutson K, Lidgren L, Robertsson O** (2009) Microbiology of the infected knee arthroplasty: Report from the Swedish Knee Arthroplasty Register on 426 surgically revised cases. Scand J Infect Dis 41:831–840.

39. **Kaplan SL** (2014) Recent lessons for the management of bone and joint infections. J Infection 68:S51–56.

40. **Schmidmaier G, Wildemann B, Stemberger A, Haas NP, Raschke M** (2001) Biodegradable poly(D,L-lactide) coating of implants for continuous release of growth factors. J Biomed Mater Res. 58:449–455.

41. **Fei J, Yu H, Pan C, Zhao C, Zhou Y, et al.** (2010) Efficacy of a norvancomycin-loaded, PDLLA-coated plate in preventing early infection of rabbit tibia fracture. Orthopedics 33:310

42. **Vester H, Wildemann B, Schmidmaier G, Stöckle U, Lucke M** (2010) Gentamycin delivered from a PDLLA coating of metallic implants: In vivo and in vitro characterisation for local prophylaxis of implant-related osteomyelitis. Injury 41:1053–1059.

43. **Greiner SH, Wildemann B, Back DA, Alidoust M, Schwabe P, et al.** (2008) Local application of zoledronic acid incorporated in a poly(D,L-lactide)-coated implant accelerates fracture healing in rats. Acta Orthop 79:717–725

44. **Grundmann S, van Royen N, Pasterkamp G, Gonzalez N, Tijsma EJ, et al.** (2007) A new intra-arterial delivery platform for pro-arteriogenic compounds to stimulate collateral artery growth via transforming growth factor-beta1 release. J Am Coll Cardiol. 50:351–358.

45. **Gollwitzer H, Thomas P, Diehl P, Steinhauser E, Summer B, et al.** (2005) Biomechanical and allergological characteristics of a biodegradable poly(D,L-lactic acid) coating for orthopaedic implants. J Orthop Res 23:802–809.

46. **Diener T** (2003) Biodegradable Drug Depots on Coronary Stents-Local Drug Delivery in Interventional Cardiology. Progress in Biomedical Research 8:82–91.

47. **Xiao L, Wang B, Yang G, Gauthier M** (2012) Poly(Lactic Acid)-Based Biomaterials: Synthesis, Modification and Applications. In: , Ghista D N(ed), . Biomedical Science, Engineering and Technology. InTech pp., 471–479.

48. **Kokai-Kun JF, Walsh SM, Chanturiya T, Mond JJ** (2003) Lysostaphin cream eradicates Staphylococcus aureus nasal colonization in a cotton rat model. Antimicrob Agents Chemother 47:1589–1597.

49. **Kokai-Kun JF, Chanturiya T, Mond JJ** (2007) Lysostaphin as a treatment for systemic Staphylococcus aureus infection in a mouse model. J Antimicrob. Chemother. 60:1051–1059.

50. **Stewart PS, Costerton JW** (2001) Antibiotic resistance of bacteria in biofilms. The Lancet 358:135–138.

51. **Høiby N, Bjarnsholt T, Givskov M, Molin S, Ciofu O** (2010) Antibiotic resistance of bacterial biofilms. Int. J. Antimicrob. Agents 35:322–332

PLosOne

Impact Factor: 3.534

5-Year Impact Factor: 4.015

80 % eigener Anteil

1. Autor und Corresponding Author

Tieroperationen, Tierbetreuung, Röntgen, Labortätigkeit